INITIAL RESULTS FOR NORTH AND SOUTH ATLANTIC SHORTFIN MAKO (*ISURUS OXYRINCHUS*) STOCK ASSESSMENTS USING THE BAYESIAN SURPLUS PRODUCTION MODEL *JABBA* AND THE CATCH-RESILIENCE METHOD *CMSY*

Henning Winker[1], Felipe Carvalho[2], Rishi Sharma[3], Denham Parker[1], and Sven Kerwath[1]

SUMMARY

*A Bayesian State-Space Surplus Production Model, JABBA, was fitted to the North and South Atlantic shortfin mako shark (*Isurus oxyrinchus*) catch and CPUE data. Results for base-case fits indicate the MSY estimate for North Atlantic was 1134.1 tons and 1130.5 tons for the South Atlantic. Stock status trajectories showed a typical anti-clockwise pattern for the North Atlantic, moving from underexploited through a period of unsustainable fishing, leading to a 99% probability of being overexploited in 2015. In contrast, the South Atlantic stock reveals a clockwise pattern moving from underexploited to a recovery state as result of decreasing biomass under sustainable fishing, which is seemingly implausible. Model diagnostics corroborated that these results were likely implausible. Results from the catch only method, CMSY, were similar to the JABBA results for North Atlantic shortfin mako shark, but strong discrepancies between CMSY and JABBA results were found for the South Atlantic. The latter can be attributed to the apparent contradiction between the observation process (i.e. CPUE) and process equation, which is informed by the catch and resilience (r) information.*

RÉSUMÉ

*Un modèle bayésien de production excédentaire état-espace, JABBA, a été ajusté aux données de capture et de CPUE du requin-taupe bleu de l'Atlantique Nord et de l'Atlantique Sud (*Isurus oxyrinchus*). Les résultats pour les ajustements du cas de base indiquent que la PME pour l'Atlantique Nord était estimée à 1.134,1 t et 1.130,5 t pour l'Atlantique Sud. Les trajectoires de l'état des stocks présentaient un schéma typique allant dans le sens inverse des aiguilles d'une montre pour l'Atlantique Nord, passant d'une sous-exploitation à une période de pêche insoutenable, conduisant à une probabilité de 99% d'être surexploité en 2015. En revanche, le stock de l'Atlantique Sud fait apparaître un schéma allant dans le sens des aiguilles d'une montre, passant d'un état sous-exploité à un rétablissement en raison de la diminution de la biomasse dans le cadre d'une pêche durable, ce qui semble improbable. Les diagnostics du modèle corroboraient que ces résultats étaient vraisemblablement improbables. Les résultats de la méthode basée uniquement sur la capture, CMSY, étaient similaires aux résultats de JABBA pour le requin-taupe bleu de l'Atlantique Nord, mais de fortes divergences entre les résultats de la CMSY et de JABBA ont été constatées pour l'Atlantique Sud. Cela peut être attribué à la contradiction apparente entre le processus d'observation (c.-à-d. CPUE) et l'équation de processus, qui est alimentée par des données de capture et de résilience (r).*

RESUMEN

Se ajustó un modelo de producción excedente bayesiano de estado espacio, JABBA, a los datos de captura y CPUE del marrajo dientuso (Isurus oxyrinchus) del Atlántico norte y sur. Los resultados para los ajustes del caso base indican que la estimación de RMS era de 1.134,1 t para el Atlántico norte y de 1.130,5 t para el Atlántico sur. Las trayectorias del estado del stock mostraban un típico patrón contrario a las agujas del reloj para el Atlántico norte, pasando de subexplotado a un periodo de pesca insostenible, que conducía a una probabilidad del 99% de estar siendo sobreexplotado en 2015. Por el contrario, el stock del Atlántico sur revela un

[1] DAFF, Department of Agriculture, Forestry and Fisheries, Private Bag X2, Rogge Bay 8012, South Africa. Email: HenningW@DAFF.gov.za
[2] NOAA Pacific Islands Fisheries Science Center, Honolulu, 1845 Wasp Boulevard, Building 176, Honolulu, Hawaii 96818.
[3] NOAA Southeast Fisheries Science Center, 75 Virginia Beach Drive, Miami, FL 33149.

patrón que sigue las agujas del reloj, pasando de una situación de subexplotación hasta una de recuperación como resultado de una biomasa descendente en el marco de una pesca sostenible, lo que aparentemente no sería plausible. Los diagnósticos del modelo corroboran que posiblemente estos resultados no son plausibles. Los resultados del método solo con capturas, CMSY, fueron similares a los resultados de JABBA para el marrajo dientuso del Atlántico norte, pero se hallaron importante discrepancias entre los resultados de CMSY y JABBA para el Atlántico sur. Esto último puede atribuirse a la aparente contradicción entre el proceso de observación (a saber, CPUE) y la ecuación del proceso, que es alimentada por la información sobre captura y resiliencia (r).

1. Introduction

In 2012, the International Commission for the Conservation of Atlantic Tunas (ICCAT) carried out the previous stock assessment for shortfin mako shark (Anon 2012), employing the Bayesian Surplus Production Model (BSP) software (Babcock and Cortes 2009). North and South Atlantic data were analyzed separately. The North Atlantic catch-per-unit-effort (CPUE) indices for the base-case were the U.S. longline logbook, Japanese longline, EU-Portugal longline and EU-Spain longline series; and catch data were available for the period 1971 to 2010. For the South Atlantic, the base case CPUE indices came from the longline fisheries of Uruguay, Japan, Brazil, EU-Portugal and EU-Spain with catch data covering the same period as for the North Atlantic. The same priors and model assumptions as for the North Atlantic were used for the South Atlantic shortfin mako stock. Specifically, the prior for intrinsic of population increase r, was assumed to be lognormally distributed with a mean of $\log(0.058)$ and a standard deviation of 0.12.

The 2012 results indicated that the status of the North and South Atlantic stocks were healthy and the probability of overfishing was low. There were, however, inconsistencies between estimated biomass trajectories, the catch series and input CPUE trends that produced wide confidence intervals in estimated trajectories and other parameters. In the North Atlantic, the model was unable to fit the U-shaped CPUE trend, which attained a minimum around 2000 and increased again until final assessment year 2010. In the South Atlantic, the increasing trend in the abundance indices since the 1970s was not biologically consistent with the increasing catches. To compensate for the increasing trend most scenarios forced the initial biomass depletion prior towards its lower bound at 0.2. However, such severely depleted stock status appears implausible given that fishing pressure prior to 1971 was most likely low in the South Atlantic. Taking into consideration results from the modeling approaches used in the assessment, the associated uncertainty, and the relatively low productivity of SMA, the Working Group recommended that the fishing mortality of shortfin mako should not be increased until more reliable stock assessment results are available for both the Northern and Southern Atlantic stocks. The high uncertainty in past catch estimates and deficiency of some important biological parameters, particularly for the southern stock, still represent obstacles for obtaining reliable estimates of current status of the stocks.

Here we present stock assessment results for the North and South Atlantic shortfin mako stock based on two approaches: (1) The Bayesian State-Space Surplus Production Model framework, JABBA (Just Another Bayesian Biomass Assessment), using updated catch and CPUE time series through 2015; and (2) the catch-only method CMSY (Froese *et al.* 2016). JABBA represents a further development of the modeling framework applied in the 2016 ICCAT South Atlantic blue shark assessment (Carvalho and Winker, 2015; Anon. 2016) and the 2017 Mediterranean Albacore assessment. The inbuilt options include: (1) automatic fitting of multiple CPUE time series and associated standard errors; (2) estimating or fixing the process variance, (3) optional estimation of additional observation variance for individual or grouped CPUE time series, and (4) specifying a Fox, Schaefer or Pella-Tomlinson production function by setting the inflection point BMSY / K and converting this ratio into shape a parameter m.

Given concerns regarding the plausibility of the simultaneously increasing trends in both catch and CPUE indices in the South Atlantic, we then explore the Monte-Carlo catch-only method CMSY (Froese et al. 2016) as alternative assessment approach for the South Atlantic SMA, while using the North Atlantic for validation purposes. CMSY builds on the Catch-MSY method put forward by Martell and Froese (2013) but addresses several shortcomings, including biased estimation of unexploited stock size and productivity, adding estimation

of biomass and exploitation rates and optimization of the underlying Monte-Carlo algorithm. These improvements have been validated against 48 simulated stocks and evaluated against 159 fully or partly assessed real stocks (Froese *et al*. 2016). The CMSY_ICCAT version presented here was developed for this study to produce assessment outputs for ICCAT.

2. Material and Methods

2.1 Fishery data

The ICCAT secretariat estimates catch for many fleets and nations based on the best available information. Catch data were revised from those used in the 2012 stock assessment. For the 2017 shortfin mako assessment, the ICCAT secretariat provided additional alternative catch times for both the North Atlantic and South Atlantic (**Figure 1**). For the North Atlantic, the updated base-case catch series starts in 1950 and the alternative catch estimates start in 1971. For the South Atlantic, the updated base-case and the alternative catch series start in 1971. For both alternative catch series, catch estimates were substantially higher during the early period of the time series 1971-1990 (**Figure 1**), but fairly similar to the base-case thereafter. For this initial assessment, we only focus on the base-case catch time series.

Catch and effort data were used to develop standardized catch-per-unit-of-effort (CPUE) time series, which were used as relative indices of abundance. CPUE was standardized for many fisheries across the North and South Atlantic Ocean. The CPUE indices considered for this assessment were based on U.S. observer, U.S. logbook, Spain longline, Japan longline and Portugal longline fisheries data for the North Atlantic and Brazil longline, Uruguay observer, Uruguay longline, Japanese longline, Spain longline and Chinese-Taipei data for the South Atlantic (**Figure 2**). In this stock assessment for SMA, all above abundance indices and associated standard errors were used to account for a full range of uncertainties about stock dynamics (**Tables 1 and 2 and Figure 2**).

2.2 JABBA Model

With JABBA we seek to improve the estimation properties of Bayesian state-space surplus production models (SPMs) by building on previous formulations by Pella and Tomlinson (1969), Gilbert (Gilbert 1992, Wang et al. 2014) and Fletcher (1978, c.f. Thorson et al. 2012). An advantage of the proposed generalization is that it links surplus production models more directly to conventional age-structured model formulations (e.g. SS3; Methot and Wetzel 2013). First we focus on the surplus production function of the generalized three parameter SPM by Pella and Tomlinson (1969):

$$(1) \qquad SP_t = \frac{r}{m-1} B_{t-1} \left(1 - \left(\frac{B_{t-1}}{K} \right)^{m-1} \right),$$

where r is the intrinsic rate of population increase at time t, K is the unfished biomass and m is a shape parameter that determines at which B/K ratio maximum surplus production is attained. If the shape parameter is $m = 2$, the model reduces to the Schaefer form, with the surplus production $g(B_t)$ attaining MSY at exactly $K/2$. If $0 < m < 2$, $g(B_t)$ attains MSY at depletion levels smaller than $K/2$ and vice versa. The Pella-Tomlinson model reduces to a Fox model if m approaches one ($m=1$) resulting in maximum surplus production at $\sim 0.37K$, but there is no solution for the exact Fox SP with $m = 1$.

B_{msy} is given by:

$$(2) \qquad B_{MSY} = K m^{\frac{-1}{m-1}},$$

and the corresponding harvest rate at MSY (H_{MSY}) is:

$$(3) \qquad H_{MSY} = \frac{r}{m-1} \left(1 - \frac{1}{m} \right),$$

where the harvest rate H is defined here as the ratio of:

$$(4) \qquad H = \frac{C}{B} \ .$$

where C denotes the catch. Correspondingly H_{MSY} can be expressed by:

$$(5) \qquad H_{MSY} = \frac{MSY}{SB_{MSY}} \ .$$

Combing and re-arranging equation (3) and (5), it follows that r in equation (1) can be expressed as:

$$(6) \qquad r = \frac{MSY}{SB_{MSY}} \frac{m-1}{1-m^{-1}}$$

or

$$(7) \qquad r = H_{MSY} \frac{m-1}{1-m^{-1}}$$

This allows re-formulating the production function of the Pella-Tomlinson equation as a function of H_{MSY}, such that:

$$(8) \qquad SP_t = \frac{H_{MSY}}{(1-m^{-1})} SB_{t-1} \left(1 - \left(\frac{B_{t-1}}{K} \right)^{m-1} \right)$$

where m can be directly translated into B_{MSY}/K and thus determines the biomass depletion level where MSY is achieved (Thorson et al. 2012), using the following relationship:

$$(9) \qquad \frac{B_{MSY}}{K} = m^{\left(-\frac{1}{m-1} \right)} .$$

Because prior formulations for most SPM-based assessments are specified for r, we provide the following equation to easily convert r estimates (or prior means) into H_{MSY} for any given shape parameter input m:

$$(10) \qquad H_{MSY} = r \frac{(m-1)}{(1-m^{-1})} .$$

However, if the prior for r is derived based on Leslie matrix approach, as commonly used for a logistic Schaefer model, we recommend approximating $H_{MSY} = r \,/\, 2$ for the purpose of comparability among Schaefer, Fox and Pella-Tomlinson production function.

Equations (5) - (10) illustrate the direct link between the Pella-Tomlinson SPM and the age-structured, which emphasizes the potential for deriving informative priors for r and m from spawning biomass- and yield-per-recruit analysis with integrated spawning recruitment relationships by generating deviates of $H_{MSY} = MSY \,/\, B_{MSY}$ and $B_{MSY} \,/\, K$, respectively (Maunder 2003, Thorson et al. 2012, Wang et al. 2014).

2.2.1 Bayesian State-Space formulation

We formulated JABBA building on the Bayesian state-space estimation framework proposed by Meyer and Millar (1999). The biomass B_y in year y is expressed as proportion of K (i.e. $P_y = B_y \,/\, K$) to improve the efficiency of the estimation algorithm.

The model is formulated to accommodate multiple CPUE series for fisheries f. The initial biomass in the first year of the time series was scaled by introducing model parameter φ to estimate the ratio of the spawning biomass in the first year to K (Carvalho et al. 2014). The stochastic form of the process equation is given by:

$$(11) \quad P_y = \begin{cases} \varphi\, e^{\eta_y} & y = 1 \\[2ex] \left[P_{y-1} + \dfrac{H_{MSY}}{(1-m^{-1})} P_{y-1}\left(1 - P_{y-1}{}^m\right) - \dfrac{\sum\limits_f C_{f,y-1}}{K} \right] e^{\eta_y} & y = 2,3,\dots,n \end{cases}$$

where η_y is the process error, with $\eta_y \sim N(0,\sigma_\eta^2)$, $C_{f,y-1}$ is the catch in year y by fishery f.

The corresponding biomass for year y is:

$$(12) \quad B_y = P_y K,$$

The observation equation is given by:

$$(13) \quad I_{f,y} = q_f B_{f,y} e^{\varepsilon_y} \qquad\qquad y = 1, 2,\dots, n.$$

where, q_f is the estimable catchability coefficient associated with the abundance index for fishery f and ε_y is the observation error, with $\varepsilon_{f,y} \sim N(0,\sigma_{\varepsilon,f,y}^2)$, where is the observation variance for fishery f in year y.

To incorporate available standard errors of the year-effect estimated from the standardization models, we modified adopted an additional variance approach for the observation error variance (Booth and Quinn 2006, Carvalho et al. 2014), such that:

$$(14) \quad \sigma_{\varepsilon,y,f}^2 = \hat{\sigma}_{SE,y,f}^2 + \sigma_{Add,f}^2 \quad \text{and} \qquad \varepsilon_{y,f} \sim N(0,\sigma_{\varepsilon,y,f}^2),$$

where $\hat{\sigma}_{SE,y,f}^2$ is the externally estimated standard error for year y and abundance index f and $\sigma_{Add,f}^2$ is the estimable additional variance.

The full Bayesian State-Space Biomass dynamics model projected over n years requires a joint probability distribution over all unobservable hyper-parameters $\boldsymbol{\theta} = \left\{ K, H_{MSY}, \varphi, \sigma_\eta^2, q_f, \sigma_{\varepsilon,y,f}^2 \right\}$ and the n process errors relating to the vector of unobserved states $\boldsymbol{\eta} = \{\eta_1, \eta_2, \dots \eta_y\}$, together with all observable data in the form of the relative abundance indices for fisheries f, $\mathbf{I}_f = \{I_{f,1}, I_{f,2}, \dots I_{f,y}\}$ (Meyer and Millar, 1999). According to Bayes' theorem, it follows that joint posterior distribution over all unobservable parameters, given the data and unknown states, can be formulated as:

$$(15) \quad \begin{aligned} p(\boldsymbol{\theta} \mid \boldsymbol{\eta}, \mathbf{I}) &= p(K)\,p(H_{MSY})\,p(\varphi)\,p(\sigma_\eta^2)\,p(q_f)\,p(q_f)\,p(\sigma_\varepsilon^2) \\ &\quad \times p(P_1 \mid \varphi, \sigma_\eta^2) \prod_{y=1}^{n} p(P_y \mid P_{y-1}, K, \varphi, \sigma_\eta^2) \times \prod_{y=1}^{n} p(I_{f,y} \mid P_t, q_f, \eta_t, \sigma_{\varepsilon,y,f}^2) \end{aligned}$$

2.2.2 JABBA prior formulations

We assumed a vaguely informative lognormal prior for K = 200,000 metric tons with a CV of 200% for both stocks. In contrast to the 2012 ICCAT shortfin mako assessment, where the same lognormal (mean = log(0.058), sd = 0.12) was assumed for the base-case scenario (Anon. 2013), we worked with different ranges of r values for the North Atlantic and South Atlantic based on recently updated life history analyses. These ranges were r_{min} = 0.01 and r_{max} = 0.06 for the North Atlantic and r_{min} = 0.03 and r_{max} = 0.09 for the South Atlantic, which were then converted in log-normal priors by:

$$(16) \quad \log(r) = \frac{r_{min} + r_{max}}{2}$$

$$(17) \quad \sigma_r = \frac{\sqrt{(\log(r) - \log(r_{\min}))^2}}{2}$$

where σ_r is the approximated lognormal standard deviation for the assumed range of r values. The corresponding lognormal priors are:

$LN \sim (\log(0.0254), 0.434)$ (*North Atlantic*)

$LN \sim (\log(0.052), 0.275)$ (*South Atlantic*)

The prior means for r were as translated into $H_{MSY} = r / 2$.

As in previous assessments, we assumed a Schaefer model for the base-case scenario by fixing input values for the shape parameter to $m = 2$. Initial depletion priors ($\varphi = B_1/K$) were inputted as means and CVs and then converted into corresponding beta priors. For our base-case scenarios, we assumed that the North Atlantic and South Atlantic stocks were fairly unexploited at the start of the catch time series in 1950 and 1971, respectively. To reflect this we assumed the same beta prior for both stocks with a mean of 0.9 and a CV of 10%. All catchability parameters were formulated as uninformative uniform priors, while the process variance and observation variance were implement by assuming inverse-gamma priors.

2.2.4 Convergence to posterior distribution

A critical issue when using MCMC methods is how to determine if random draws have converged to the posterior distribution. Convergence of the MCMC samples to the posterior distribution was checked by monitoring the trace and by diagnosing the autocorrelation plot. Gelman and Rubin (1992) and Heidelberger and Welch (1983) diagnostics as implemented in the R language (R Development Core Team, 2013) and the CODA package were also examined. In this study, three MCMC chains were used. The model was run for 100,000 iterations, sampled with a thinning rate of 10 with a burn-in period of 20,000 for each of the three chains. Basic diagnostics of model convergence and fitting included visualization of the MCMC chains, comparing the predicted CPUE indices for each model to the observed CPUE and inspecting the process error deviation over time.

2.2.5 Performance diagnostics and prediction properties

As additional model performance diagnostics we applied a jackknife procedure and prediction-validation, including a visual inspection of the retrospective patterns. For the jackknife, we focused on the relative influence of individual CPUE series by removing one at a time and predicting the stock status in the form of B / B_{MSY} and H / H_{MSY} trajectories. For the prediction-validation, we iteratively excluded the last ten years of CPUE observations, refitted the model and projected forward until the final year 2015. During each backward-iteration, all CPUE observations were removed at once for the respective year. The retrospectives were visualized by only showing projections for the next year instead of projecting all the way forward to the final year 2015.

2.3 Catch and resilience method CMSY

Typically, production models rely on time series of catch and CPUE to estimate productivity. Instead, the CMSY method uses catch and productivity to estimate biomass, exploitation rate, MSY, and related fisheries reference points as well as the resilience of the species from catch data. In doing so, CMSY provides an alternative assessment tool for situations where CPUE indices are not available or potentially unreliable. Assuming underlying population dynamics of the Schaefer Model, probable ranges of parameters r and K are filtered with a Monte-Carlo algorithm to detect 'viable' r-K pairs. A parameter pair is considered 'viable' if the corresponding biomass trajectories are compatible with the observed catches in the sense that predicted biomass does not become negative, and is compatible with prior estimates of relative biomass ranges for the beginning and the end of the respective time series. As such, CMSY builds on the concepts Catch-MSY method of Martell and Froese (2013). Perhaps the most important achievement of CMSY compared with the Catch-MSY method of Martell and Froese (2013) lies in overcoming the problems created by a triangular rather than ellipsoid distribution of the viable r-k pairs as a result of the Monte-Carlo filtering procedure. Other improvements include adding estimation of biomass and exploitation rates as standard CMSY output and the implementation of a Bayesian state-space Schaefer surplus production model (CMSY.BSM) as routine tool within the CMSY software (Froese *et al.* 2016). Froese *et al.* (2016) demonstrated that the tip of the triangle typically transverses the expected ellipsoid

cloud of viable *r-K* pairs found by fitting an implemented Bayesian state-space Schaefer surplus production model (CMSY.BSM) to catch and abundance data. Froese et al. (2016) validated CMSY against 48 simulated stocks and evaluated against 159 fully or partly assessed real stocks, which suggested that CMSY provides a fairly robust tool for data-limited assessments given the limited input requirements.

During the development of CMSY software, special emphasis was given to derive informative priors for productivity, unexploited stock size, catchability and biomass from population dynamics theory (see Froese et al. 2006 for details). Both CMSY and CMSY.BSM can incorporate three uniform prior ranges for *B/K* at the beginning and end of the time series, and optionally also in an intermediate year. Poorly specified biomass depletion priors resulting from the default rules, such as setting initial biomass to medium when instead the stock was still lightly exploited or already severely depleted at the beginning of the time series can lead to erroneous conclusions regarding the current stock status. Gross misspecifications are often identifiable by unrealistically "forced" trajectories and a lack of viable *r-K* pairs. A detailed discussion on risk of circularity and general guidelines for specifying depletion priors is provided in Froese et al. (2016).

2.3.1 CMSY_ICCAT

For the purpose of this assessment, we developed an "ICCAT-friendly" version (CMSY_ICCATv2.R) for the original CMSY R code by Froese et al. (2016) to facilitate comparison of CMSY results with outputs of conventionally used Bayesian surplus models. Among the newly implemented features are: (1) a plot comparing normalized trends of CMSY biomass projection to observed and predicted CPUE from the CMSY.BSM, (2) plots comparing CMSY distributions for *K*, *r*, B_{cur}/B_{MSY} and F_{cur}/F_{MSY} to the corresponding posteriors from the CMSY.BSM, as well as priors for *K* an *r* and (3) a Kobe-type biplot that allows comparing the CMSY and CMSY.BSM trajectories of the ratios F/F_{MSY} (y-axis) over B/B_{MSY} (x-axis), with uncertainties for the assessment year final illustrated as kernel density plots denoting the 50%, 80% and 95% credibility intervals. Note that $F = H = C/B$ is used interchangeable in this study. The original CMSY version by Froese et al. (2016) applies a Schaefer model that is modified to account for impaired recruitment by resembling a hockey-stick function of B/B_{MSY}. Although this adjustment has showed several merits (Froese et al. 2016), for the purpose of comparability, the current version CMSY_ICCATv2.R (https://github.com/Henning-Winker/CMSY-ICCAT) applies a conventional Schaefer model at this stage.

2.3.2 CMSY and CMSY.BSM priors

The productivity parameter *r* is inputted into CMSY as a min/max range, which is then converted into lognormal priors by applying Equations (16) – (17) (Froese *et al.* 2016). These priors are then passed on to CMSY and CMSY.BSM. For the purpose of comparability, we used the same *r* ranges as for the JABBA

The CMSY framework allows setting depletion priors (*B/K*) for the start, middle and end of the time series, which are mainly required for CMSY. For the purpose of this explorative assessment, we assumed the same informative *B/K* prior uniform prior range for the first year as $B_{start}/K = 0.85$-0.99 and vaguely to moderately informative prior ranges for the intermediate $B_{int}/K = 0.3$ - 0.9 and final year 2015 $B_{end}/K = 0.1$ - 0.8. The only difference between the North and South Atlantic was setting the intermediate year to 1990 and 1995, respectively. These years were choosen to be positioned after the first peak in each of the catch time series, which appeared lagged by approximately 5 years for the South Atlantic (Figure 1). Setting this prior in this way is based on the assumption that the biomass of a slow growing species such as shortfin mako should be at least depleted by 10% following the first substantial increase in catches.

3. Results and Discussion

3.1 JABBA model outputs

3.1.1. Convergence of base-case models

All JABBA model runs showed robust convergence diagnostics. The visual inspection of trace plots of the major parameters showed good mixing of the three chains (i.e., moving around the parameter space), which is a first indication of convergence of the MCMC chains (**Figures A1-A2**). The Heidelberger and Welch test could not reject the hypothesis that the MCMC chains were stationary at the 95% confidence level for any of the estimable parameters. Overall, these diagnostics indicated that the posterior distribution of the model parameters was adequately sampled.

3.1.2. CPUE fits

The predicted CPUE indices for base-case models were compared to the observed CPUE to determine model fit. The North Atlantic shortfin mako stock assessment base-case model fits to CPUE are shown in Figure 3. In general, the predicted CPUE fluctuated around the observed CPUE time series for all the indices included in the model and the underlying trends in observed and predicted CPUE were notably consistent. By contrast, the South Atlantic base-case model fits revealed clear lack of fit (**Figure 4**), in particular for the Japanese and Brazilian indices, and there was overall considerable noise in the data.

3.1.3 Posterior estimates of model parameters

Plots of posterior densities for the North and South Atlantic base-case model parameters are shown in **Figure 5** and **Figure 6**, together with their respective prior densities (shown for informative priors only). Summaries of posterior quantiles of parameters and quantities of management interest are presented in **Table 1.**

For the North Atlantic base-case, the marginal posterior for r has a median of about 0.030 (0.012 - 0. 075% C.I.), which closely approximated the prior. As for the North Atlantic, the posterior of r for the South Atlantic closely approximated the prior (**Figures 5 and 6**). The considerable overlap between prior and posterior densities could indicate that the r estimates may be largely informed by their priors.

The posterior for K for the North Atlantic had a median of 171,179.5 metric tons (85,411.1 – 480,171.7 95% C.I.), while the estimated median for the South Atlantic was approximately half with 83,163.1 metric tons (45,226.0 – 173,471.3 95% C.I.). The relatively narrow density of the K posteriors compared to their prior indicated that the posteriors for both stocks were strongly informed by the data (**Figures 5 and 6**).

The marginal posteriors for initial (deterministic) depletion was similar for both stocks with median estimates of 0.88 in 1950 for the North Atlantic and 0.82 in 1970 for the South Atlantic **(Table 1)**. As for the estimate of r, the large overlap between the prior and posterior estimates indicated limited information and therefore high uncertainty for this estimate (**Figures 5 and 6**). This situation was aggravated for the South Atlantic, where the spread of the posterior density exceeded the prior substantially. This may be indicative of model misspecification. Similarly, the process error was estimated to be notable smaller for the North Atlantic (median = 0.105) than for the South Atlantic (median = 1.126).

3.1.4 Reference points and stock status

The *MSY* estimate for North Atlantic base-case was estimated at 1134.1 metric tons (479.9 – 3324.5 95% C.I.) and at 1130.5 metric tons (325.3 – 2274.1 95% C.I.) for the South Atlantic. The relatively small difference in MSY despite a substantially higher K estimate for the North Atlantic can be largely attributed to relatively lower r estimate for the North Atlantic, given that r and K are strongly interrelated. This also translates directly into H_{MSY}, being directly proportional to r when assuming the Schaefer production function.

Stock depletion (*B/K*) and status estimates (*B /BMSY* and *H / H_{MSY}*) are provided together with the model parameter estimates in **Table 1**. The North Atlantic base-case JABBA predicts severe biomass depletion at 26.9% of pristine levels (*K)* for the final assessment year 2015, with the range of 95% credibility intervals of *B / K* = 12.2 – 46.3% falling entirely below B_{MSY}. The base-case scenario for the South Atlantic produces a n more optimistic estimate of *B / K* = 70.5% (43.1% - 93.4% 95% C.I.), albeit associated with considerable uncertainty.

The predicted *H / H_{MSY}* trajectories for North Atlantic base-case run would imply that sustainable harvest rates were already exceeded by 1985, peaked in 1995 at around five times higher than the sustainable level and then stabilized at around four times higher than sustainable levels over the period 2000-2015 (**Figure 7**). The corresponding *B / B_{MSY}* trajectory implies a steep decline since 1985, a relative minimum at around 2000, followed by a moderate increase until 2010 and subsequent decrease to the current level at approximately 50% of B_{MSY}.

Similar to the North Atlantic, the predicted *H / H_{MSY}* trajectories for South Atlantic base-case run shows a steadily increasing, fluctuating trend, which started to become consistently unsustainable around 1995, peaked around 2005 and then shows a slight decline to about 1.7 times the sustainable level by 2015 (**Figure 8**). Contrary to the North Atlantic, the corresponding *B / B_{MSY}* trajectory shows a substantial recovery from 1985 onwards to levels at 40% above B_{MSY} in 2015, which followed an initial rapid depletion period of below B_{MSY} between 1970 and 1985 (**Figure 8**). The initial depletion to levels below B_{MSY} under a sustainable harvest regime

in the South Atlantic, followed by a complete recovery under a highly unsustainable fishing regime, points towards a severe contradiction between the state process in the form of catch and resilience (r) information and the observation process in the form of CPUE data.

The simultaneous development of the B/B_{MSY} and H/H_{MSY} is illustrated by means of Kobe biplots for the North (**Figure 9**) and South (**Figure 10**) Atlantic base-case runs. The Kobe plot for the North Atlantic shows a typical anti-clockwise pattern with the stock status moving from underexploited through a period of unsustainable fishing, leading to a 99% posterior probability of being over-exploited in 2015. Contrary to population theory, the South Atlantic stock reveals a clockwise pattern moving from an underexploited state to a recovery as result of decreasing biomass under sustainable fishing, which is followed by a short period of overfishing before a biomass rebuilding phase during the recent period of unsustainable harvest rates above H_{MSY}. The resulting stock status posterior for 2015 therefore appears both implausible and ambiguous, with 4.6% support for an overfished state (red), 16% for a sustainable stock (green) and 79.4% (yellow) of the posterior pairs falling within the area of unsustainable harvesting ($H/H_{MSY} > 1$ and $B/B_{MSY} > 1$), despite an extended period of biomass increase in recent years.

3.1.5 Jackknife, Prediction Validation and Retrospectives

The jackknife procedure demonstrated that the base-case run for the North Atlantic was fairly insensitive to excluding any one CPUE series at a time, as this resulted in hardly discernable effects on the predicted CPUE and the stock status trajectories of B/B_{MSY} and H/H_{MSY} (**Figure 11**). The jackknife procedure conducted for the South Atlantic base-case scenario showed that removing the Uruguay LL data had the strongest effect on the predicted CPUE and B/B_{MSY}, whereas H/H_{MSY} was fairly insensitive to removing any of the available CPUE time series (**Figure 12**). The second strongest effect was achieved by excluding the Japanese CPUE data. Although this effect was manifested in the predicted CPUE and B/B_{MSY} over the early time period (1970-1987), it had fairly little impact on the stock status for the final assessment year 2015 (**Figure 12**).

The retrospective pattern for the North Atlantic model appeared robust and indicates that the JABBA would have been able to accurately determine the stock status back to 2010 (**Figure 13**). The South Atlantic base-case runs, however, showed strong retrospective patterns, which notably affected B/B_{MSY} but to a lesser extent H/H_{MSY} (**Figure 14**). Similar to the Jackknife procedure, the strong retrospective pattern on B/B_{MSY} suggest undesirable model performance for the South Atlantic.

The prediction validation for the North Atlantic base-case suggests that the prediction capacity of the JABBA fit is sufficiently robust to adequately forecast the stock status over time periods of up to eight years, with high accuracy possible over a period of three years (**Figure 15**). Comparable to the jackknife procedure and retrospectives inference, the base-case JABBA for the South Atlantic showed adequate forecasting properties for H/H_{MSY}, whereas the prediction validation for B/B_{MSY} showed again poor performance (**Figure 16**).

In summary, the North Atlantic base-case JABBA performed well against all three applied model diagnostic procedures. By contrast, the South Atlantic base-case JABBA indicated substantially poorer performance with regards to the robustness of estimates and forward projections of B/B_{MSY}, whereas H/H_{MSY} estimates and forward projection properties were found to be fairly robust.

3.2 CMSY results

A comparison between CMSY and the CMSY.BSM fitted to US logbook CPUE and North Atlantic catch data (1950-2015) is illustrated in **Figures 17-19**. While there are notable differences in the interrelated estimates of r and K (**Figures 17 and 18**), there is general agreement for the 2015 estimates of F/F_{MSY} (i.e. H/H_{MSY}) and B/B_{MSY} (**Figures 18 and 19**) and similar trends in the long-term trajectories, albeit with some intermittent divergences in the B/B_{MSY} trajectory. This similarity between CMSY, CMSY.BSM and JABBA further corroborates the North Atlantic CPUE indices can be adequately described by the underlying population dynamics, given the catch input and the prior specification for r for SMA in the North Atlantic.

Although the CMSY and CMSY.BSM estimates of r and K are more similar for the South Atlantic (**Figure 20**) than for the North Atlantic, the 2015 estimates for F / F_{MSY} (i.e. H / H_{MSY}) and B / B_{MSY} were in poor agreement. The CMSY results suggest that the South Atlantic stock status is as pessimistic as that of the North Atlantic (**Figures 21 and 22**). The strong discrepancy between and the fitted models and CMSY, which is independent of CPUE, further highlights that the CPUE-driven stock status estimates for the South Atlantic should be treated with caution.

3.3 Stock Assessment implications for Atlantic shortfin mako shark

The overall good fits and promising performance properties for the North Atlantic base-case scenario indicates that JABBA provides a promising framework for fitting multiple and highly variable, but informative CPUE time series within a Surplus Production Model framework. The probabilistic interpretation of stock status suggested an overfished stock status of North Atlantic shortfin mako, which is exposed to highly unsustainable harvest rates.

In contrast, the evaluation of the South Atlantic base-case model is much more ambiguous. Based on the applied diagnostics, our estimates of unsustainable harvest rates in the South Atlantic appear to be fairly robust, whereas the biomass depletion and B/B_{MSY} estimates are highly uncertain. This was further corroborated by the good agreement between the catch-only method CMSY and JABBA results for North Atlantic, but strong discrepancies between CMSY and JABBA results for the South Atlantic. We suggest that the latter can be largely attributed to the apparent contradiction between the observation process (i.e. CPUE) and process equation, which is informed by the catch and resilience (r) information.

Literature cited

Anon 2013. Report of the 2012 Shortfin Mako Stock Assessment and Ecological Risk Assessment Meeting (Olhão, Portugal - June 11-18, 2012). ICCAT. Col. Vol. Sci. Papers. 69 (4): 1427-1570.

Anon 2016. Report of the 2015 Blue Shark Stock Assessment (Oceanário de Lisboa, Lisbon, Portugal – 27-31 July 2015). Col. Vol. Sci. Pap. 72(4): 866-1019.

Babcock, E.A. and Cortes, E. 2009, Updated Bayesian Surplus Production Model applied to blue and mako shark catch, CPUE and effort data. Collect. Vol. Sci. Pap. ICCAT 64(5): 1568-1577.

Carvalho, F., and Winker, H. 2016. Stock assessment of south Atlantic blue shark (*Prionace glauca*) through 2013. ICCAT document SCRS/2015/153.

Carvalho, F., Ahrens, R., Murie, D., Ponciano, J.M., Aires-da-silva, A., Maunder, M.N., and Hazin, F. 2014. Incorporating specific change points in catchability in fisheries stock assessment models : An alternative approach applied to the blue shark (*Prionace glauca*) stock in the South Atlantic Ocean. Fish. Res. 154: 135–146.

Fletcher, R.1978. On the restructuring of the Pella–Tomlinson system. Fish. Bull. 76: 515–512.

Froese, R., Demirel, N., Coro, G., Kleisner, K.M., and Winker, H. 2016. Estimating fisheries reference points from catch and resilience. Fish Fish 83: 506–526

Gelman, A., and Rubin, D. B. 1992. Inference from Iterative Simulation Using Multiple Sequences. Statistical Science 7: 457-472.

Gilbert. 1992. A stock production modelling technique for fitting catch histories to stock index data.

Heidelberger, P., and Welch, P. D. 1983. Simulation Run Length Control in the Presence of an Initial Transient.

Martell, S., and Froese, R. 2013. A simple method for estimating MSY from catch and resilience. 505: 504–514.

Maunder, M.N. 2003. Is it time to discard the Schaefer model from the stock assessment scientist's toolbox? Fish. Res. 61: 145–149.

Methot, R.D., and Wetzel, C.R. 2013. Stock synthesis: A biological and statistical framework for fish stock assessment and fishery management. Fish. Res. 142: 86–99.

Meyer, R., and Millar, R. B. 1999. BUGS in Bayesian stock assessments. Canadian Journal of Fisheries and Aquatic Sciences 56: 1078–1087.

Pella, J.J., and Tomlinson, P.K. 1969. A generalized stock production model. Inter-American Trop. Tuna Comm. Bull. 13: 421–458.

Thorson, J.T., Cope, J.M., Branch, T.A., and Jensen, O.P. 2012. Spawning biomass reference points for exploited marine fishes, incorporating taxonomic and body size information. Can. J. Fish. Aquat. Sci. 69: 1556–1568.

Wang, S.-P., Maunder, M.N., and Aires-da-Silva, A. 2014. Selectivity's distortion of the production function and its influence on management advice from surplus production models. Fish. Res. 158: 181–193.

Table 1. Summary of posterior quantiles of parameters from the JABBA base-case fits to North Atlantic and South Atlantic SMA catch and CPUE series.

Estimates	North Atlantic			South Atlantic		
	Median	2.50%	97.50%	Median	2.50%	97.50%
K	171179.5	85411.1	480171.7	83163.1	45226.0	173471.3
r	0.030	0.012	0.075	0.056	0.032	0.094
$\psi\,(psi)$	0.888	0.602	0.995	0.826	0.380	0.992
σ	0.105	0.084	0.134	0.126	0.095	0.176
H_{MSY}	0.015	0.006	0.038	0.039	0.01	0.056
B_{MSY}	85589.8	42705.5	240085.8	30082.7	18104.5	59737.5
MSY	1344.1	479.9	3324.5	1130.5	325.3	2274.1
B_{1950}/K	0.838	0.57	1.047	0.84	0.612	1.067
B_{2015}/K	0.269	0.122	0.468	0.706	0.43	0.93
B_{2015}/B_{MSY}	0.537	0.245	0.937	1.412	0.861	1.861
H_{2015}/H_{MSY}	4.616	1.894	11.878	1.745	0.790	6.254
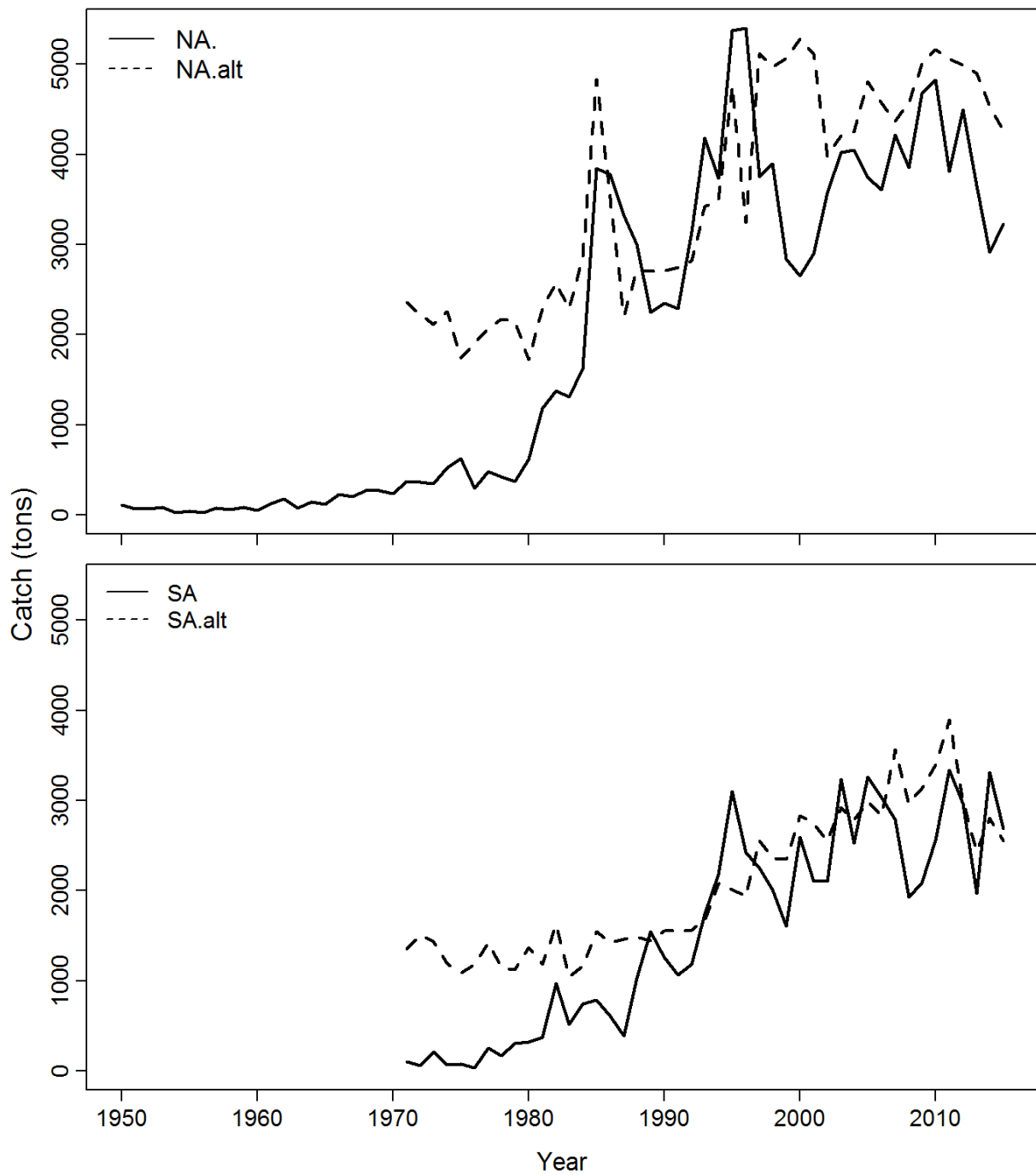
Figure 1. Time-series of catch (metric tons) for the shortfin mako shark in the North Atlantic (NA) and South Atlantic (SA). The solid line denotes the base-case scenario used in this assessment, while the dotted line represents an alternative reconstructed catch series estimate.
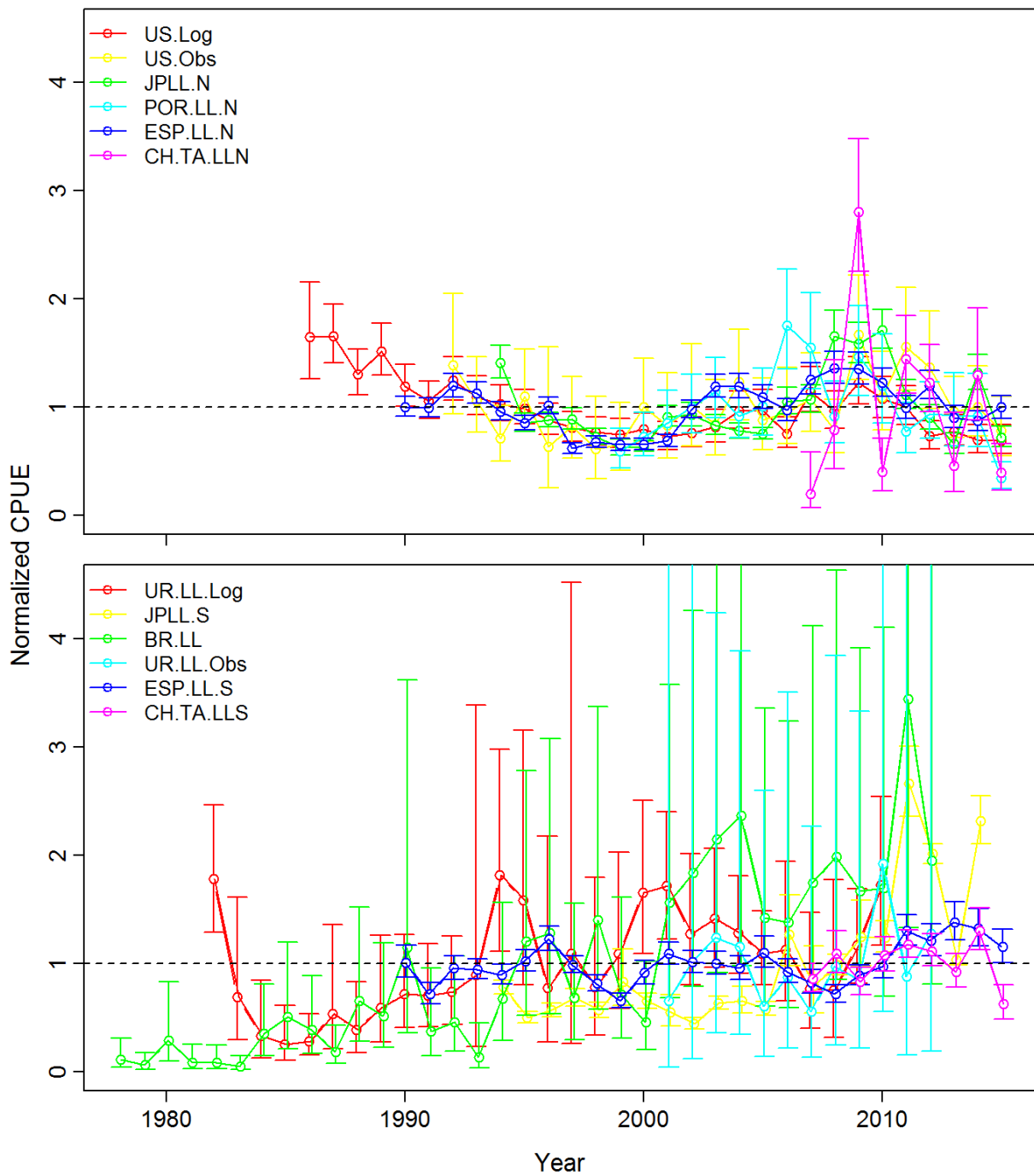
Figure 2. Time-series of five standardized CPUE series for the shortfin mako shark in the North Atlantic (upper panel) and South Atlantic (lower panel), with error bars denoting the standard errors associated with the CPUE estimates.
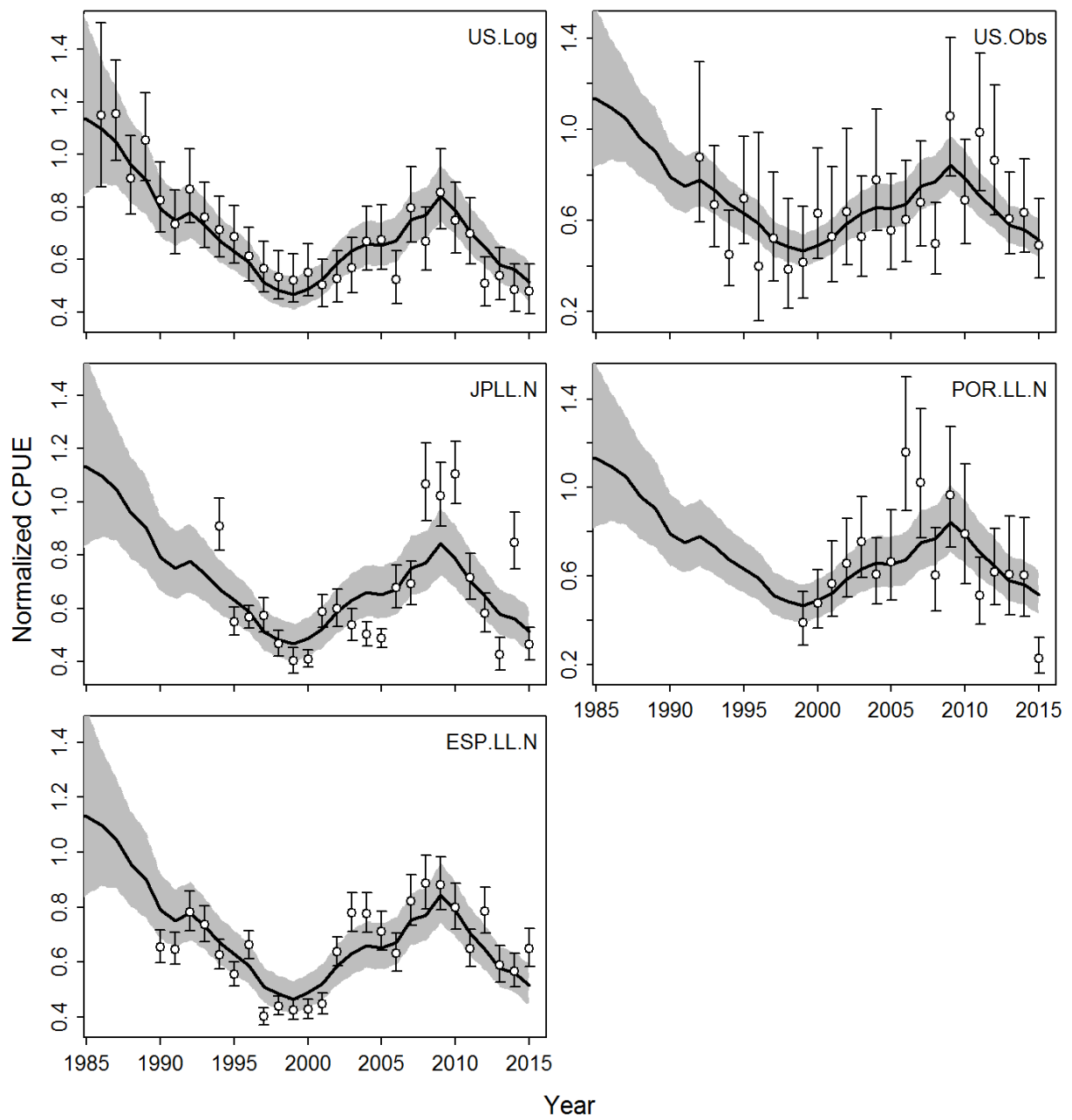
Figure 3. JABBA fits of time-series of observed (circle) and predicted (solid line) catch-per-unit-effort (CPUE) for the North Atlantic shortfin mako shark base-case scenario. Shaded grey area indicates 95% C.I.
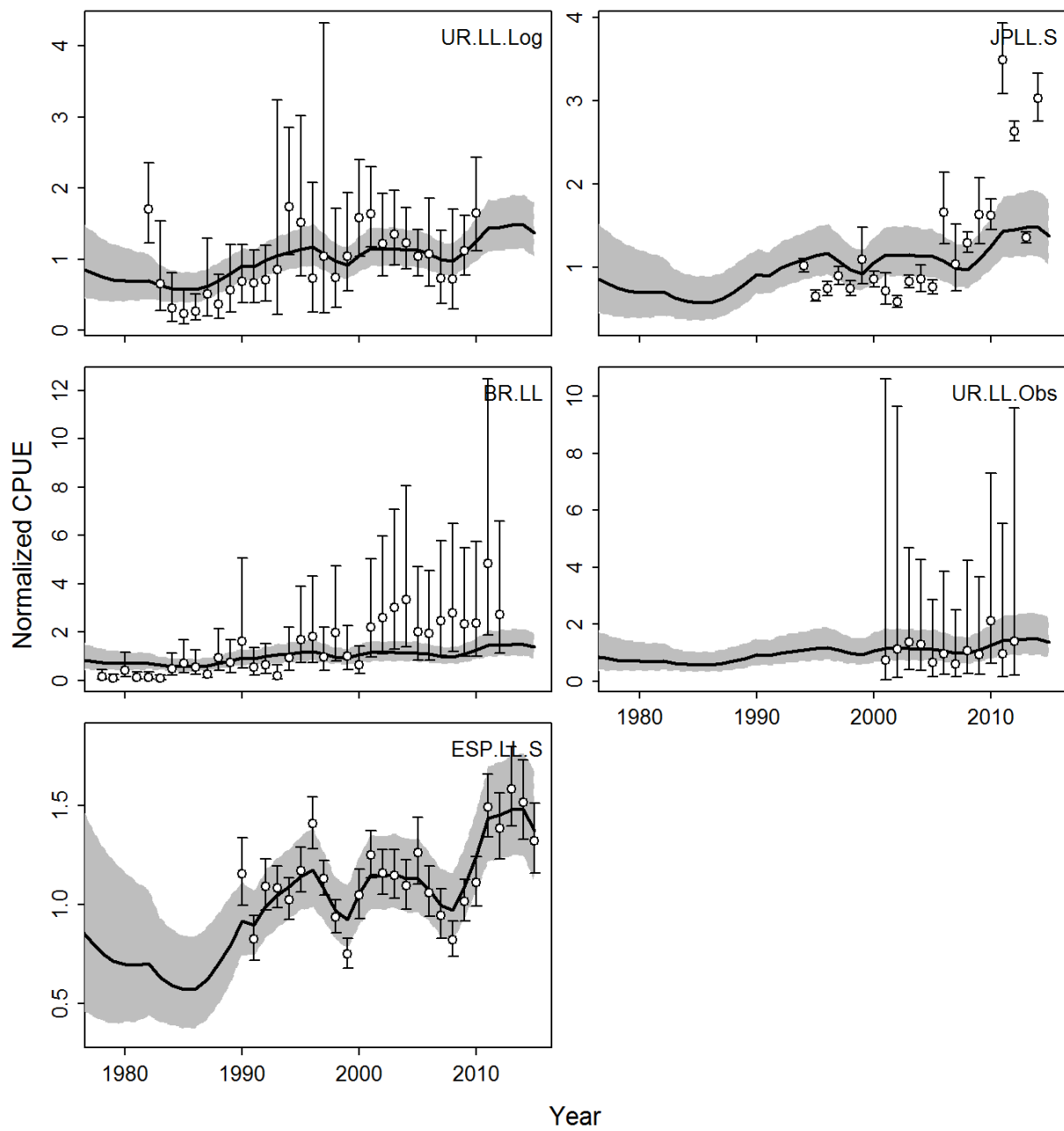
Figure 4. JABBA fits of time-series of observed (circle) and predicted (solid line) catch-per-unit-effort (CPUE) for the South Atlantic shortfin mako shark base-case scenario. Shaded grey area indicates 95% C.I..
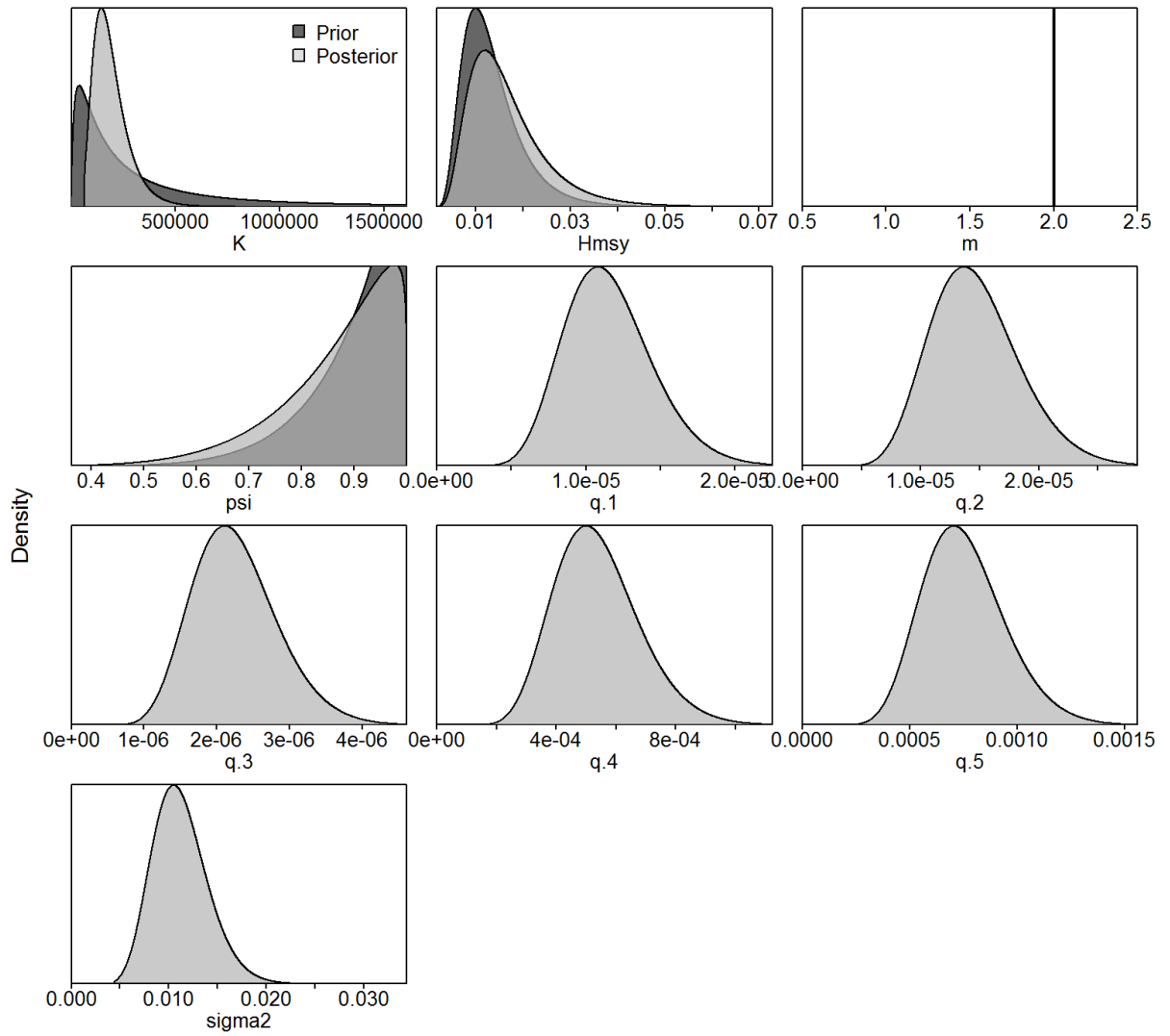
Figure 5. Prior and posterior distributions for base-case scenario of the North Atlantic shortfin mako shark stock assessment.
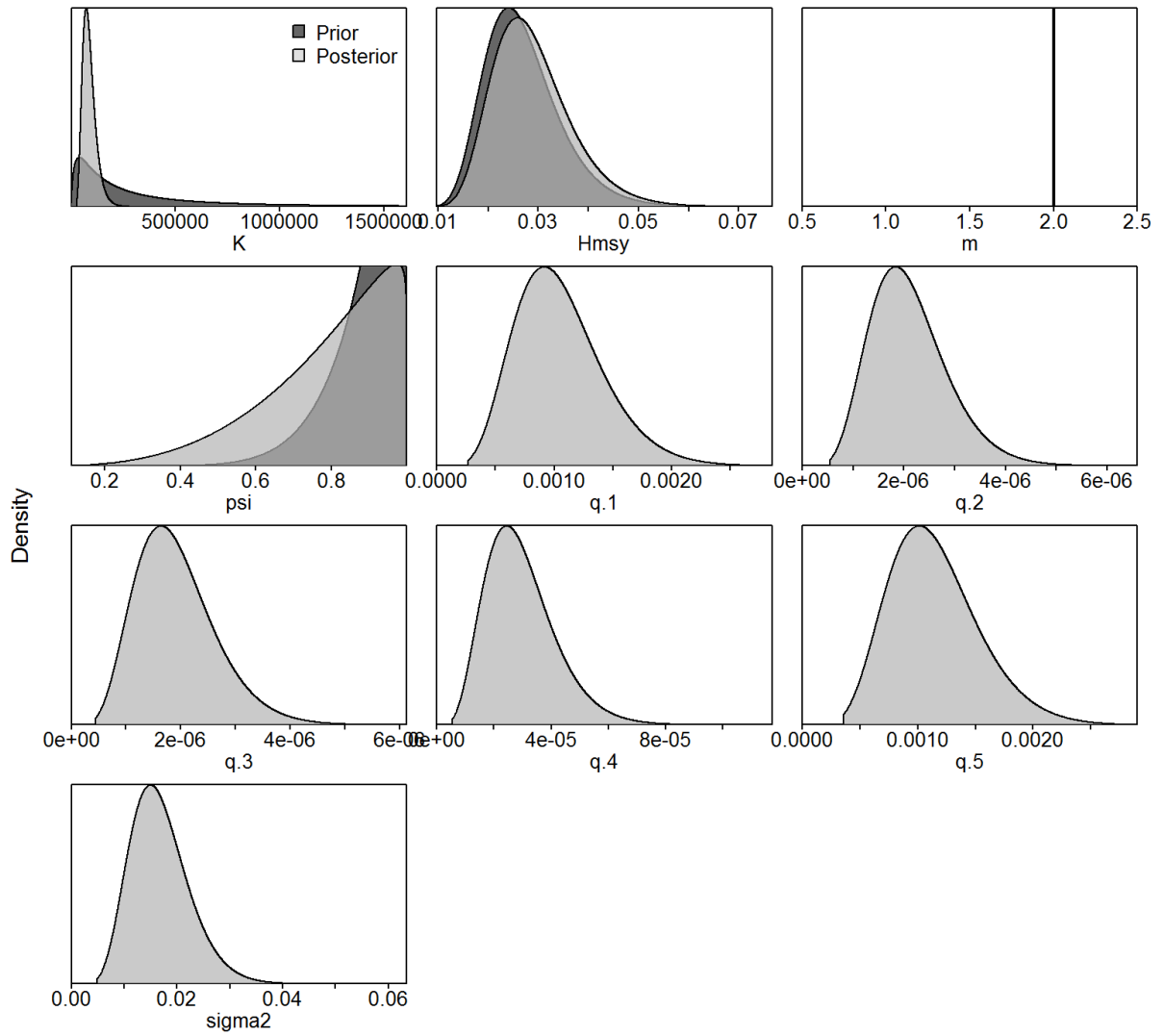
Figure 6. Prior and posterior distributions for base-case scenario of the South Atlantic shortfin mako shark stock assessment.
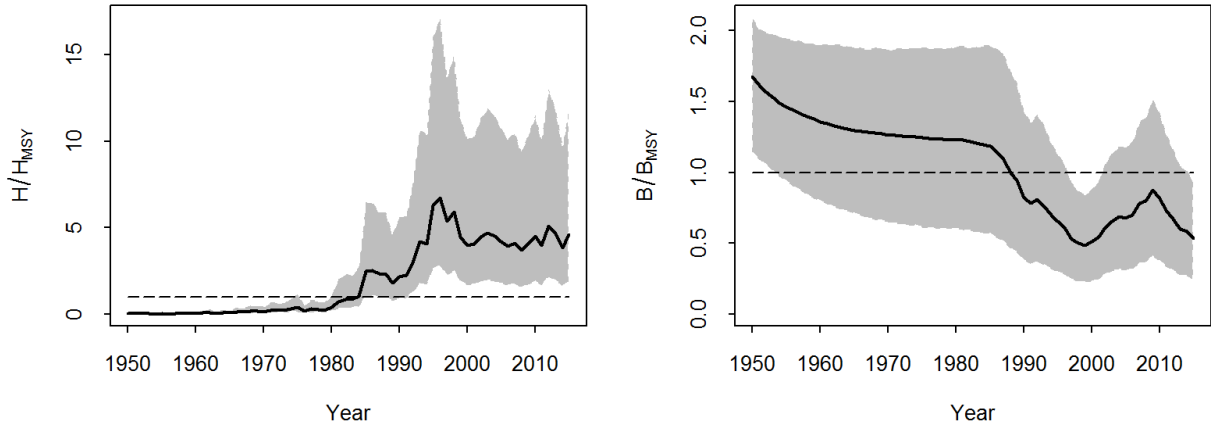
Figure 7. Trends in harvest rate relative to H_{MSY} and biomass relative to B_{MSY} for the period 1950-2015 for the North Atlantic shortfin mako shark stock assessment base-case.
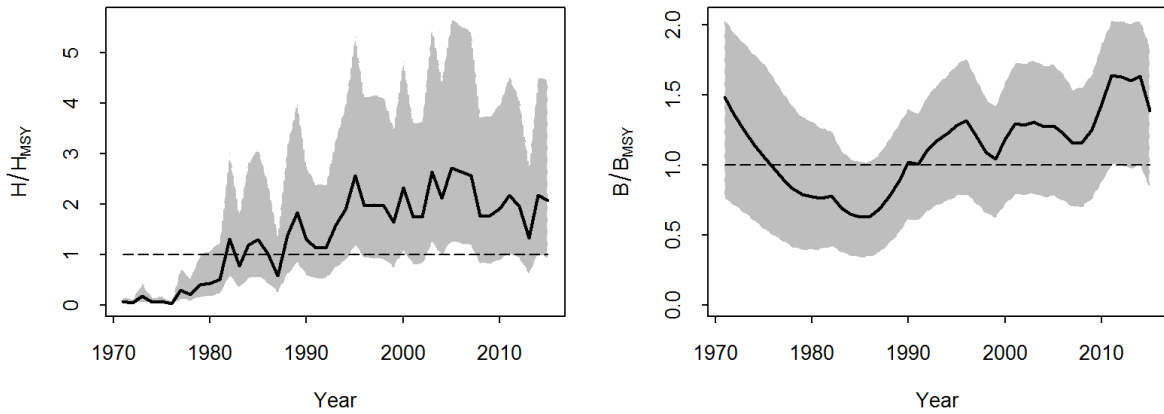
Figure 8. Trends in harvest rate relative to H_{MSY} and biomass relative to B_{MSY} for the period 1970-2015 for the South Atlantic shortfin mako shark stock assessment base-case.
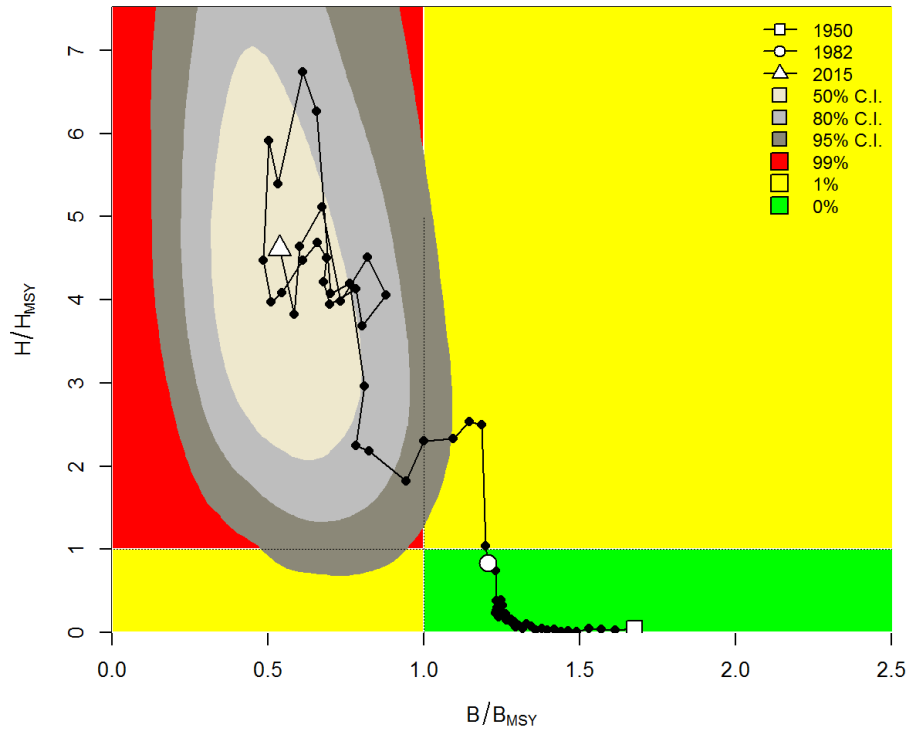
Figure 9. Kobe diagram showing the estimated trajectories (1950-2015) of B/B$_{MSY}$ and H/H$_{MSY}$ for the base-case scenario for the North Atlantic shortfin mako shark stock assessment. Different grey shaded areas denote the 50%, 80% and 95% credibility interval for the final assessment years.
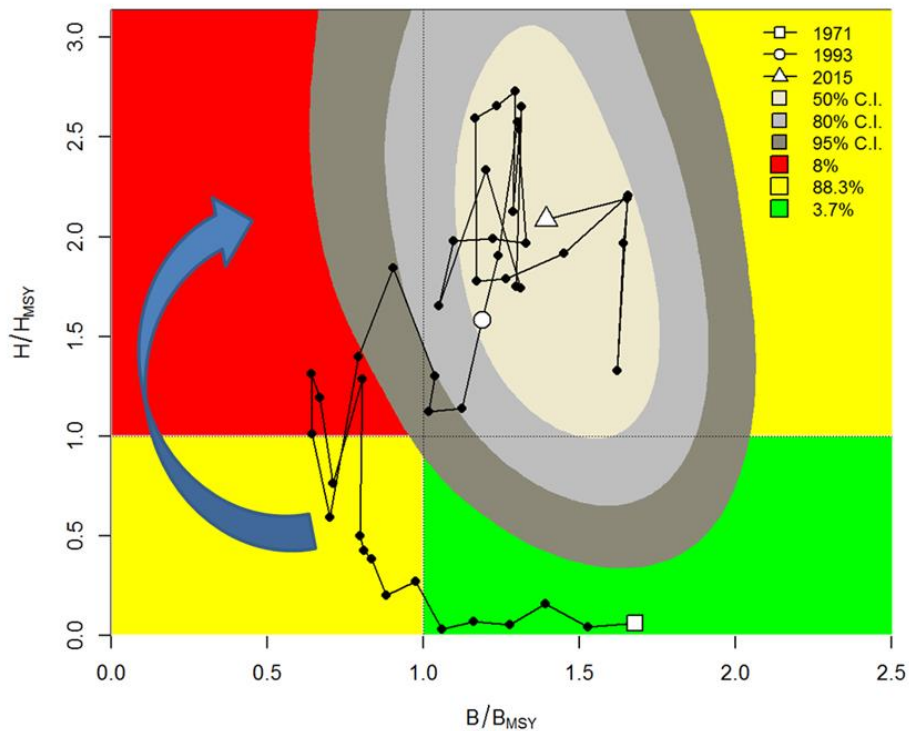
Figure 10. Kobe diagram showing the estimated trajectories (1950-2015) of B/B$_{MSY}$ and H/H$_{MSY}$ for the base-case scenario for the South Atlantic shortfin mako shark stock assessment. Different grey shaded areas denote the 50%, 80% and 95% credibility interval for the final assessment years. The blue arrow highlights implausible clockwise pattern moving from an underexploited state to a recovery as result of decreasing biomass under sustainable fishing, which is followed by a short period of overfishing.
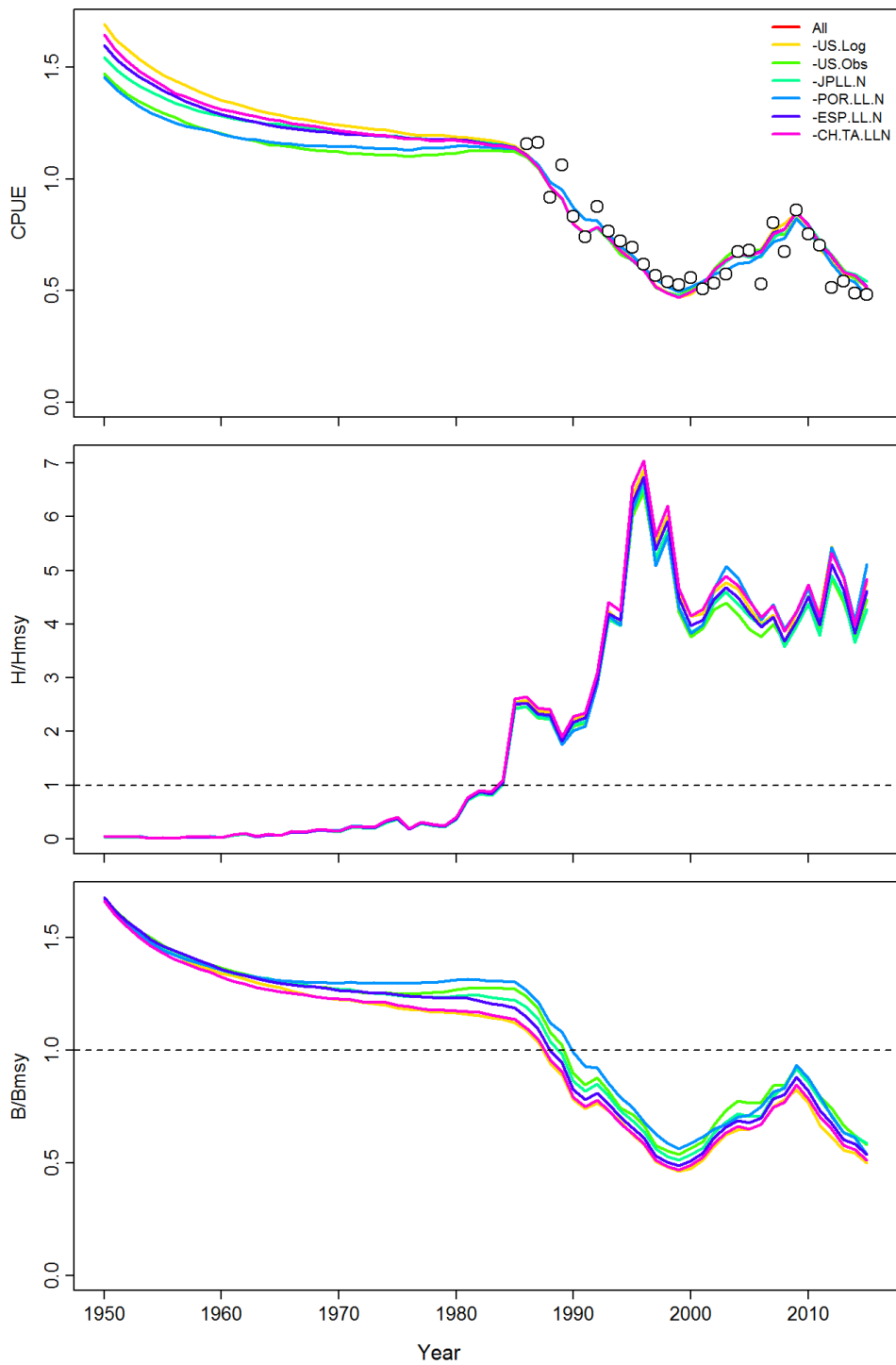
Figure 11. Jackknife diagnostics with respect to the CPUE series, F/F_{MSY} and B/B_{MSY} over time for the North Atlantic base-case scenario, with open circles illustrating the US LL CPUE.
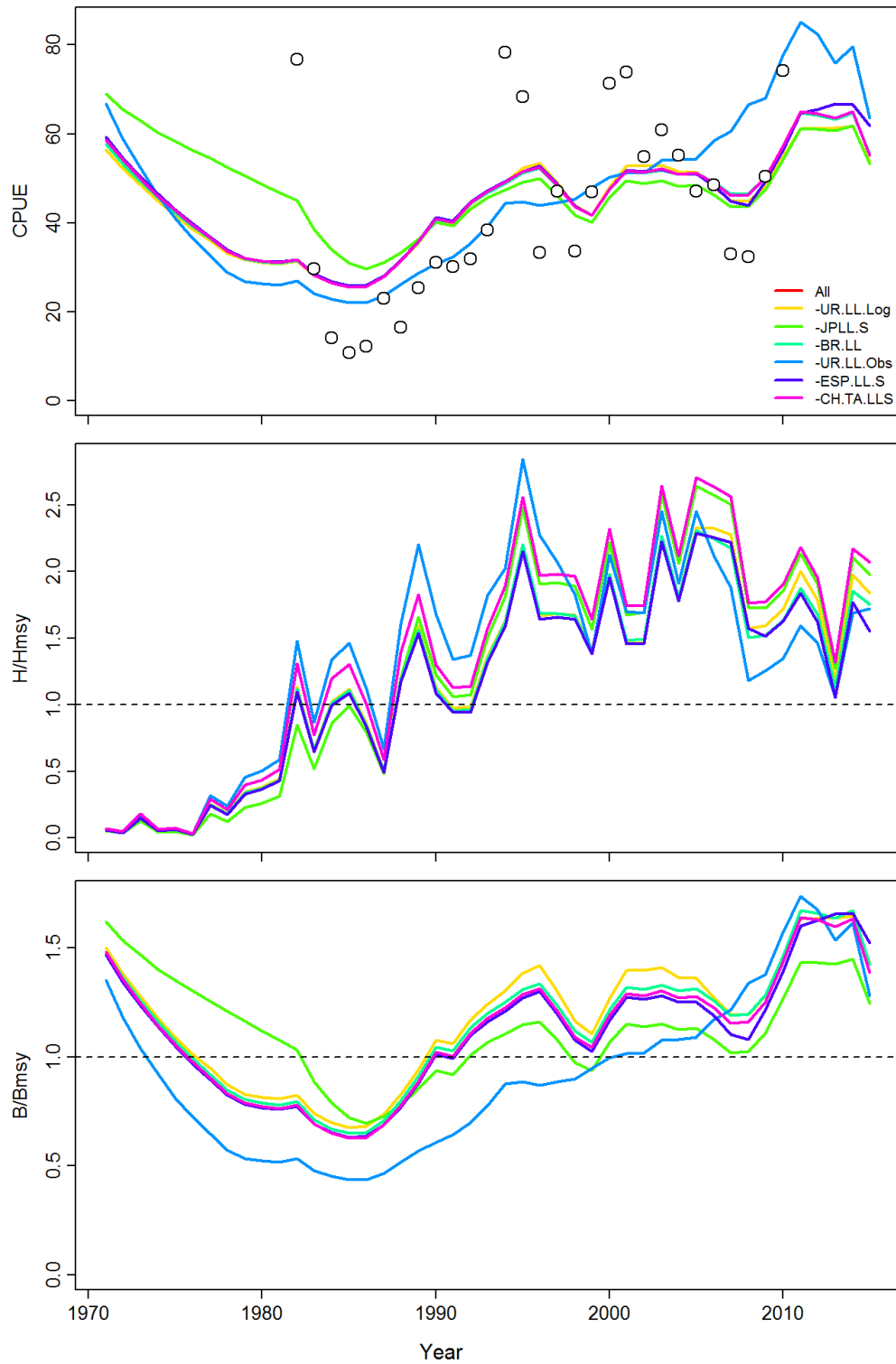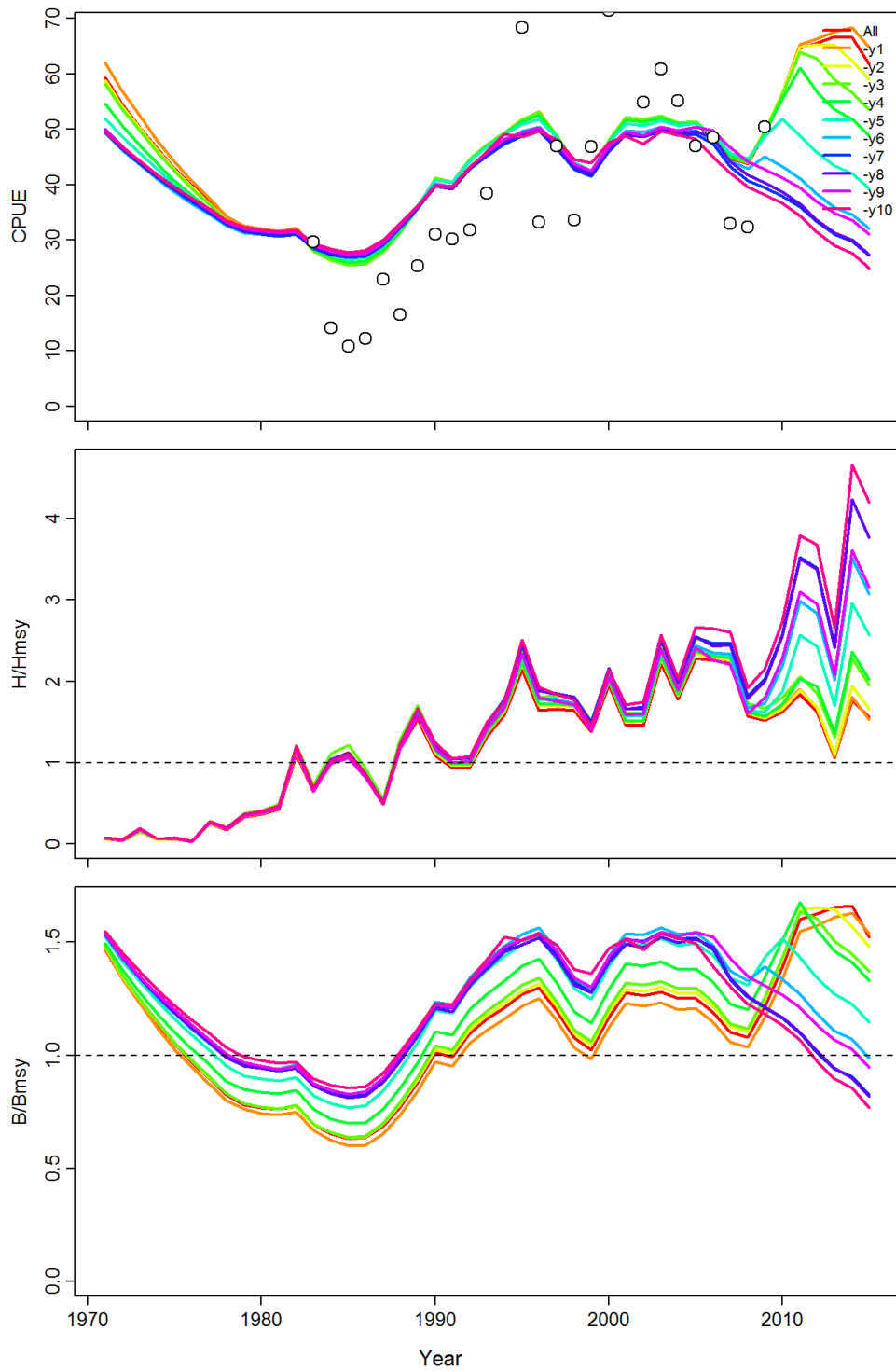
Figure 12. Jackknife diagnostics with respect to the CPUE series, F/F_{MSY} and B/B_{MSY} over time for the South Atlantic base-case scenario, with open circles illustrating the Brazilian LL CPUE.
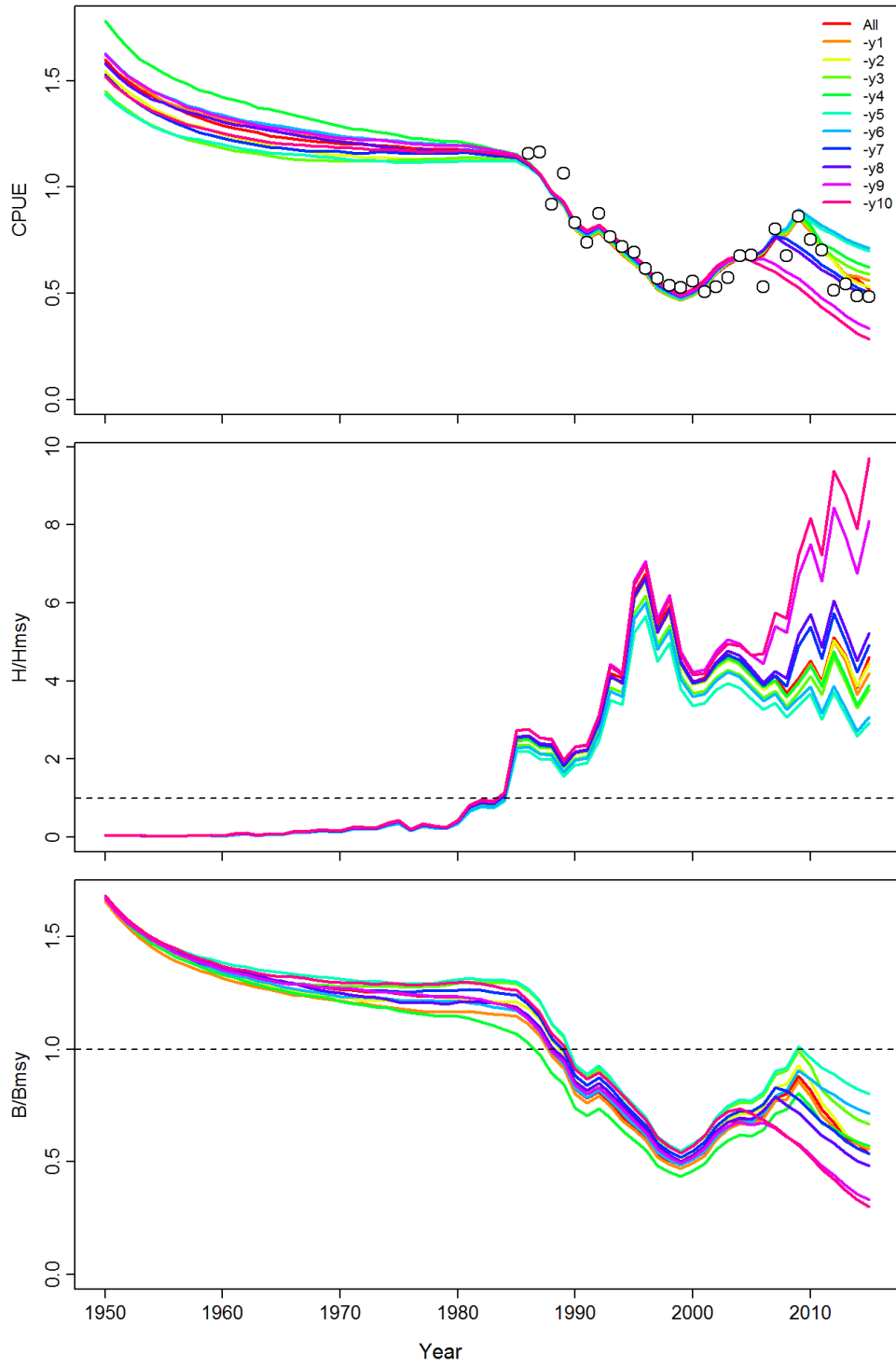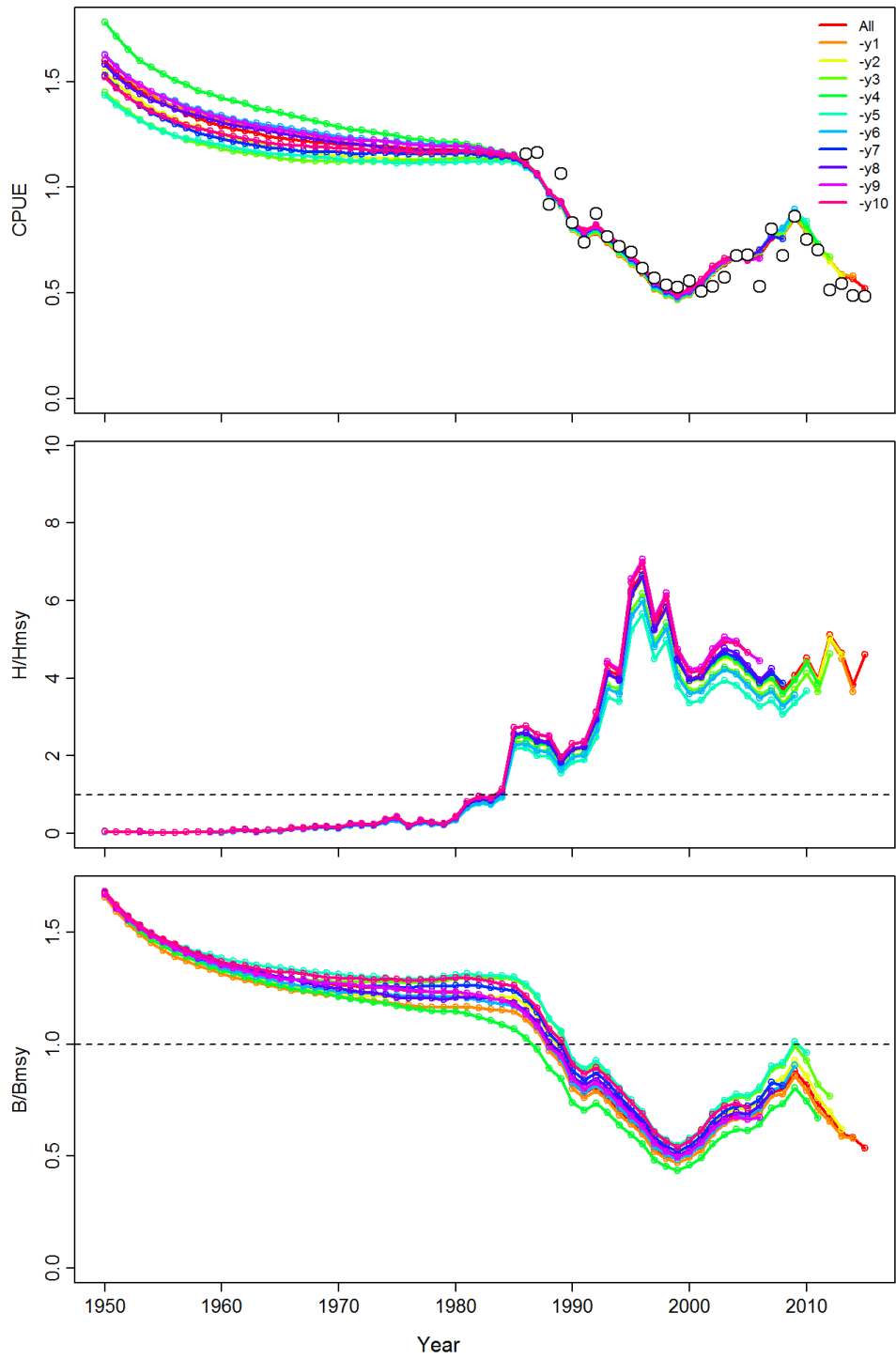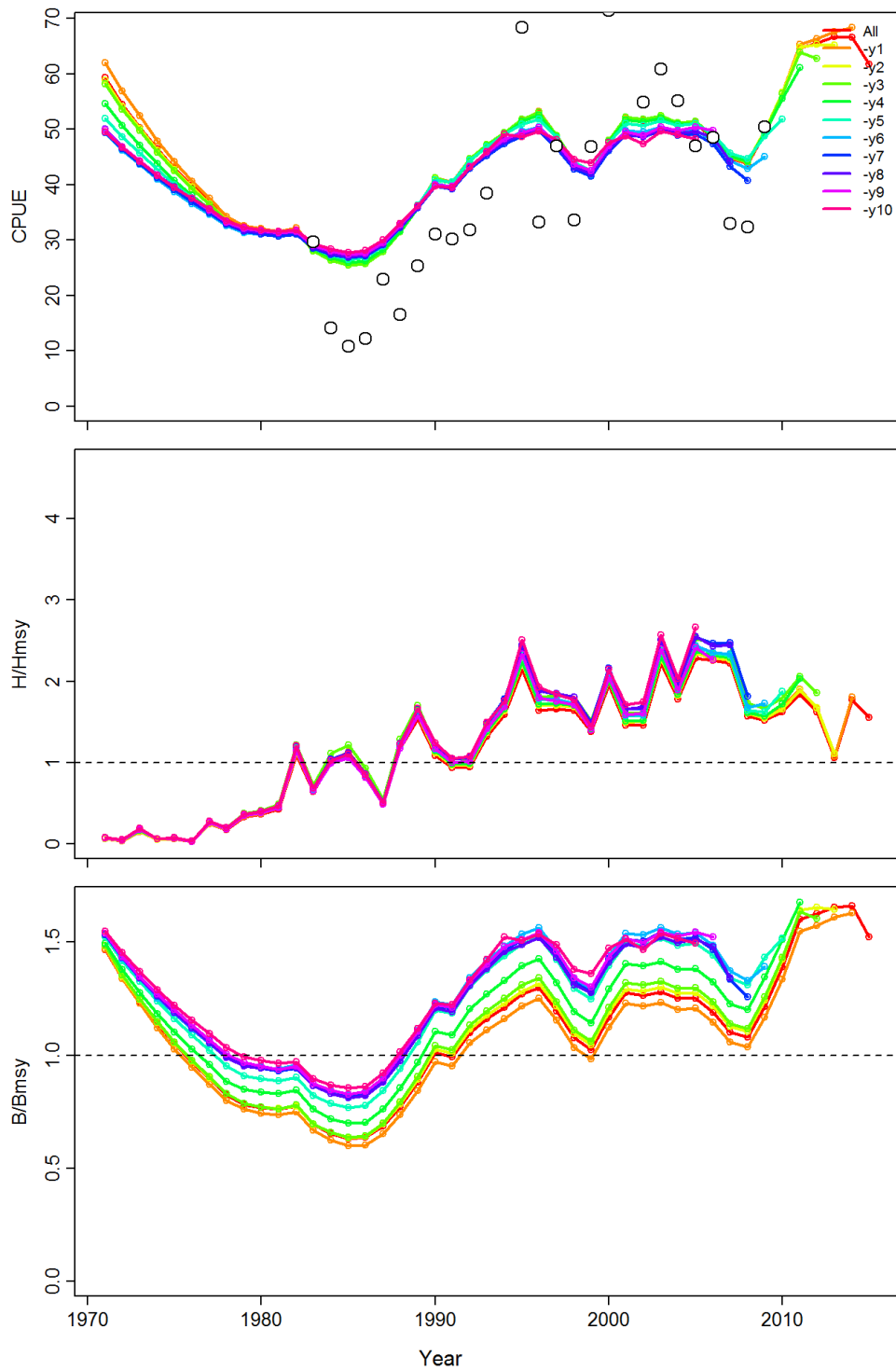
Figure 13. Cross-validation prediction diagnostics with respect to the CPUE series, H / H_{MSY} and B/B_{MSY} over time for the North Atlantic base-case scenario, with open circles illustrating the US LL CPUE.

Figure 14. Cross-validation prediction diagnostics with respect to the CPUE series, H / H$_{MSY}$ and B/B$_{MSY}$ over time for the South Atlantic base-case scenario, with open circles illustrating the Brazilian LL CPUE.

Figure 15. Retrospective diagnostics with respect to the CPUE series, H / H_{MSY} and B/B_{MSY} over time for the North Atlantic base-case scenario, with open circles illustrating the US LL CPUE.

Figure 16. Retrospective diagnostics with respect to the CPUE series, H / H_{MSY} and B/B_{MSY} over time for the South Atlantic base-case scenario, with open circles illustrating the Brazilian LL CPUE.
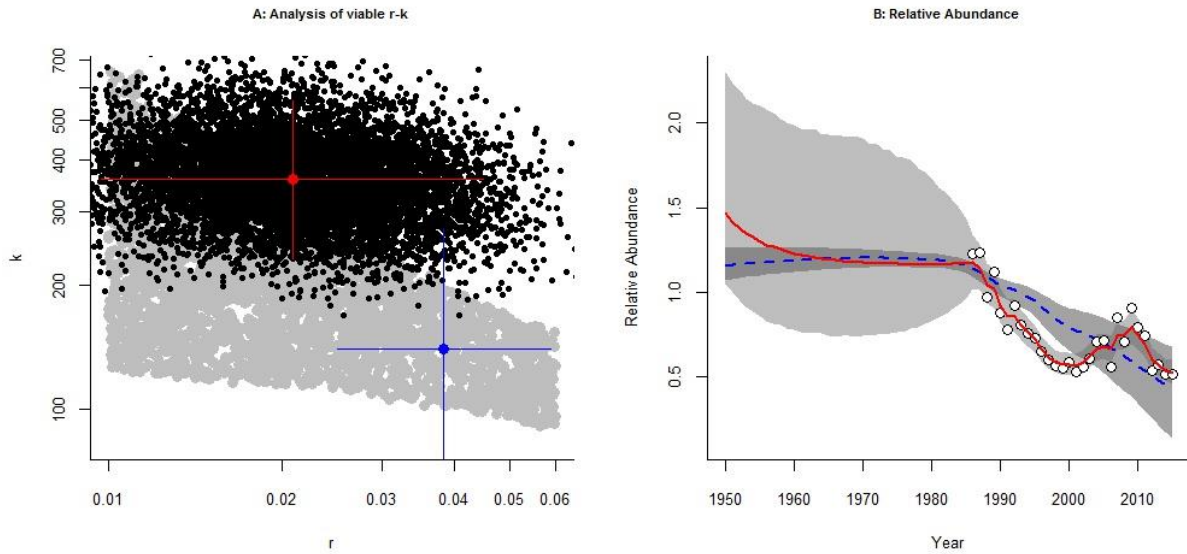
Figure 17. Comparison of CMSY and CMSY_BSM for the North Atlantic SMA base-case, showing (**A**) viable r-K pairs from CMSY (grey dots) and r-K posterior values (black dots), with indication of approximate 95% credibility intervals denoted by the blue crosshair for CMSY and the red crosshair the CMSY.BSM model and (**B**) a comparison of the normalized projected biomass trend from CMSY with observed and predicted CPUE values fitted with CMS.BSM to US logbook long-line CPUE.
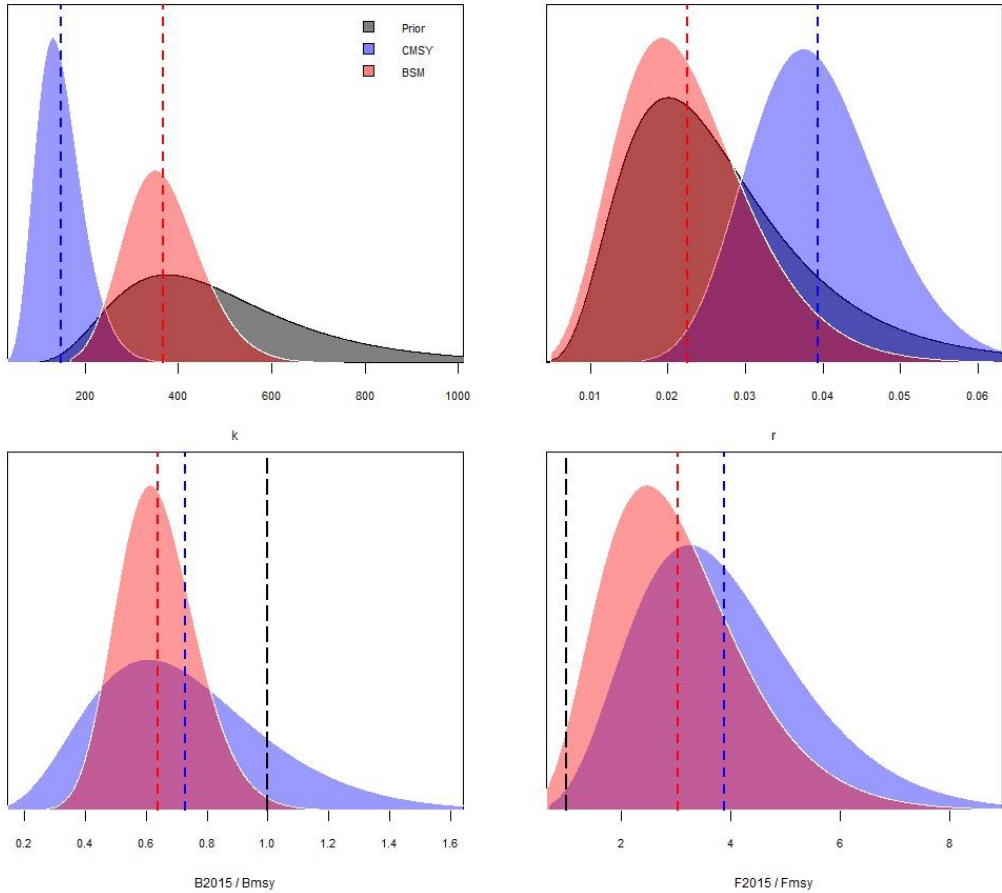
Figure 18. Comparison of CMSY (blue) and CMSY.BSM (red) for the North Atlantic SMA base-case, showing r and K posterior densities relative to their priors (upper panel) and posterior densities for B_{2015}/B_{MSY} and F_{2015}/F_{MSY} relative to their MSY reference (black dashed line). Note that F is used here interchangeable with harvest rate H = C/B.
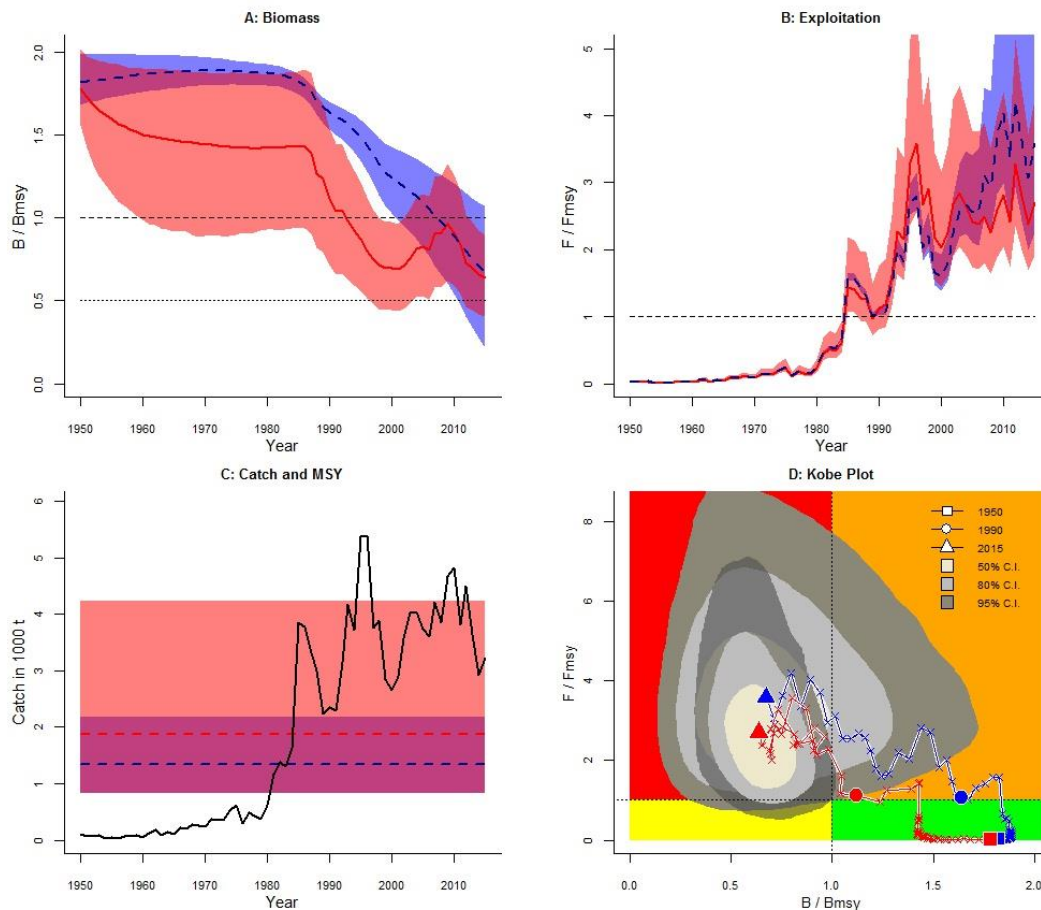
Figure 19. Comparison of CMSY (blue) and CMSY_BSM (red) for North Atlantic SMA showing the trajectories of (**A**) predicted B / B$_{MSY}$ (**B**) predicted F / F$_{MSY}$ (**C**) catches superimposing the MSY region (95% CIs) and (**D**) kobe-type biplot with uncertainty for the final year illustrated by kernel densities. Note that F is used here interchangeable with harvest rate H = C/B.
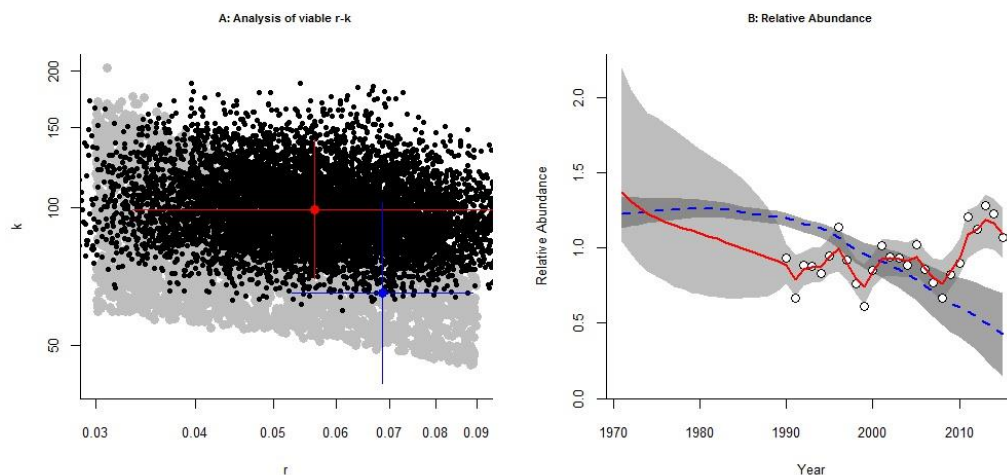

Figure 20. Comparison of CMSY and CMSY_BSM for the South Atlantic SMA base-case, showing (**A**) viable r-K pairs from CMSY (grey dots) and r-K posterior values (black dots), with indication of approximate 95% credibility intervals denoted by the blue crosshair for CMSY and the red crosshair the CMSY.BSM model and (**B**) a comparison of the normalized projected biomass trend from CMSY with observed and predicted CPUE values fitted with CMS.BSM to US logbook long-line CPUE.
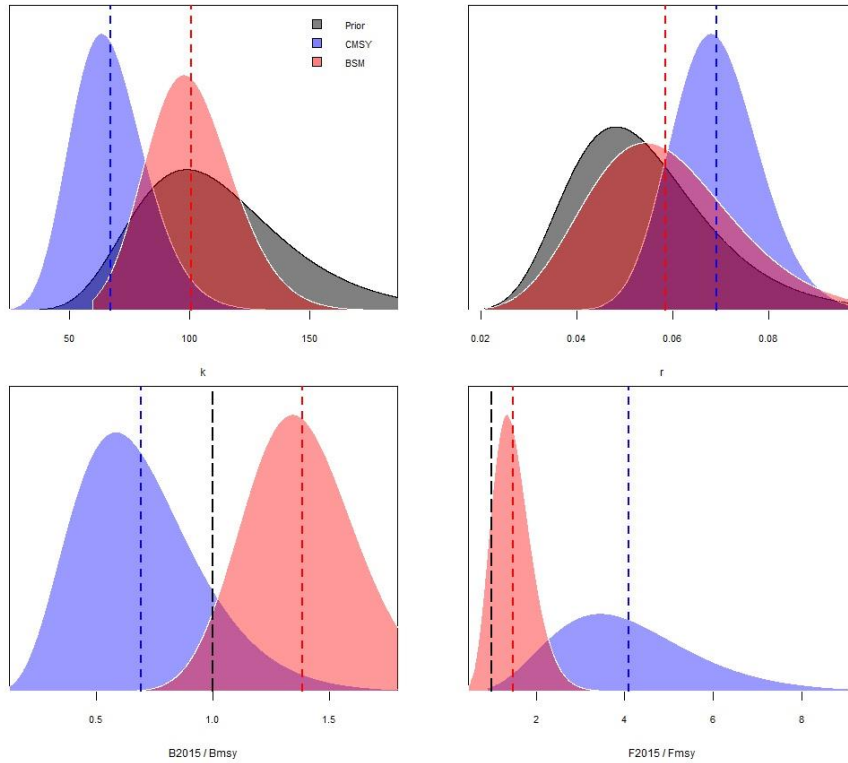
1863

Figure 21. Comparison of CMSY (blue) and CMSY.BSM (red) for the South Atlantic SMA base-case, showing r and K posterior densities relative to their priors (upper panel) and posterior densities for B_{2015} / B_{MSY} and F_{2015} / F_{MSY} relative to their MSY reference (black dashed line). Note that F is used here interchangeable with harvest rate H = C/B.
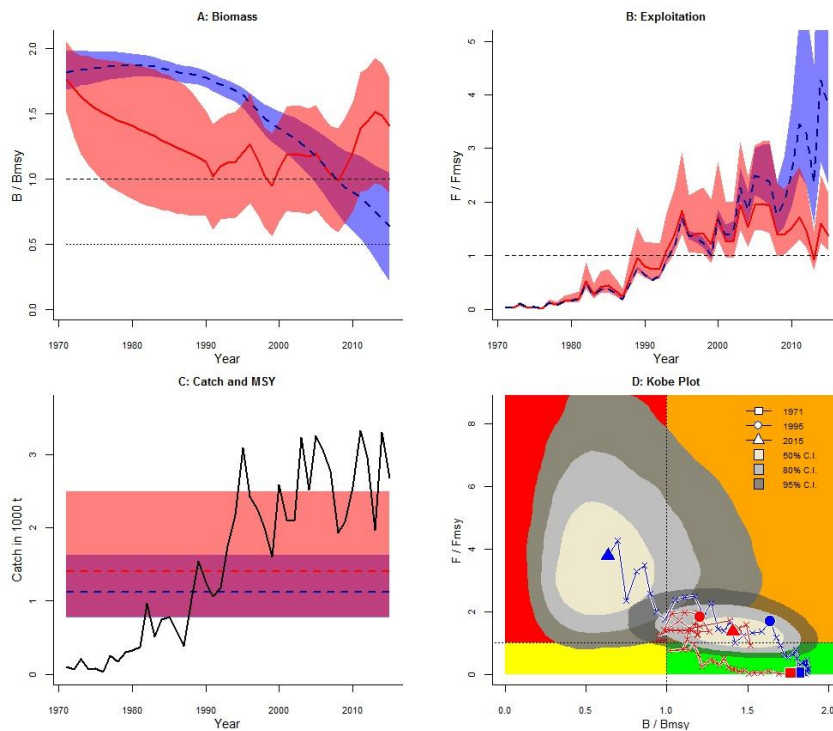

Figure 22. Comparison of CMSY (blue) and CMSY_BSM (red) for South Atlantic SMA showing the trajectories of (**A**) predicted B / B_{MSY} (**B**) predicted F / F_{MSY} (**C**) catches superimposing the MSY region (95% CIs) and (**D**) Kobe-type bi-plot with uncertainty for the final year illustrated by kernel densities. Note that F is used here interchangeable with harvest rate H = C/B.

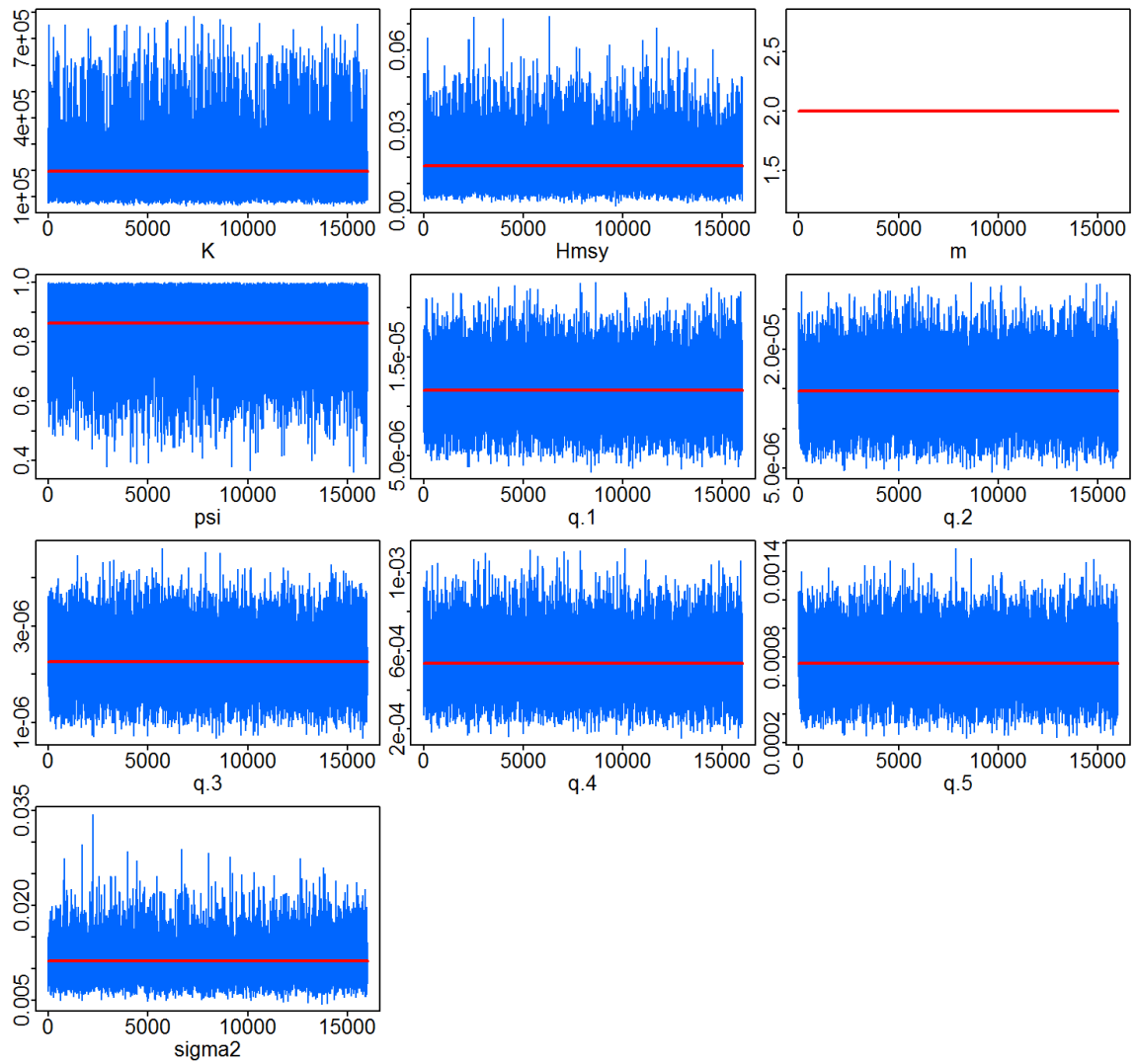**Figure A1.** Trace plots for the main model parameter drawn from MCMC samples in the base-case scenario for North Atlantic shortfin mako shark stock assessment.
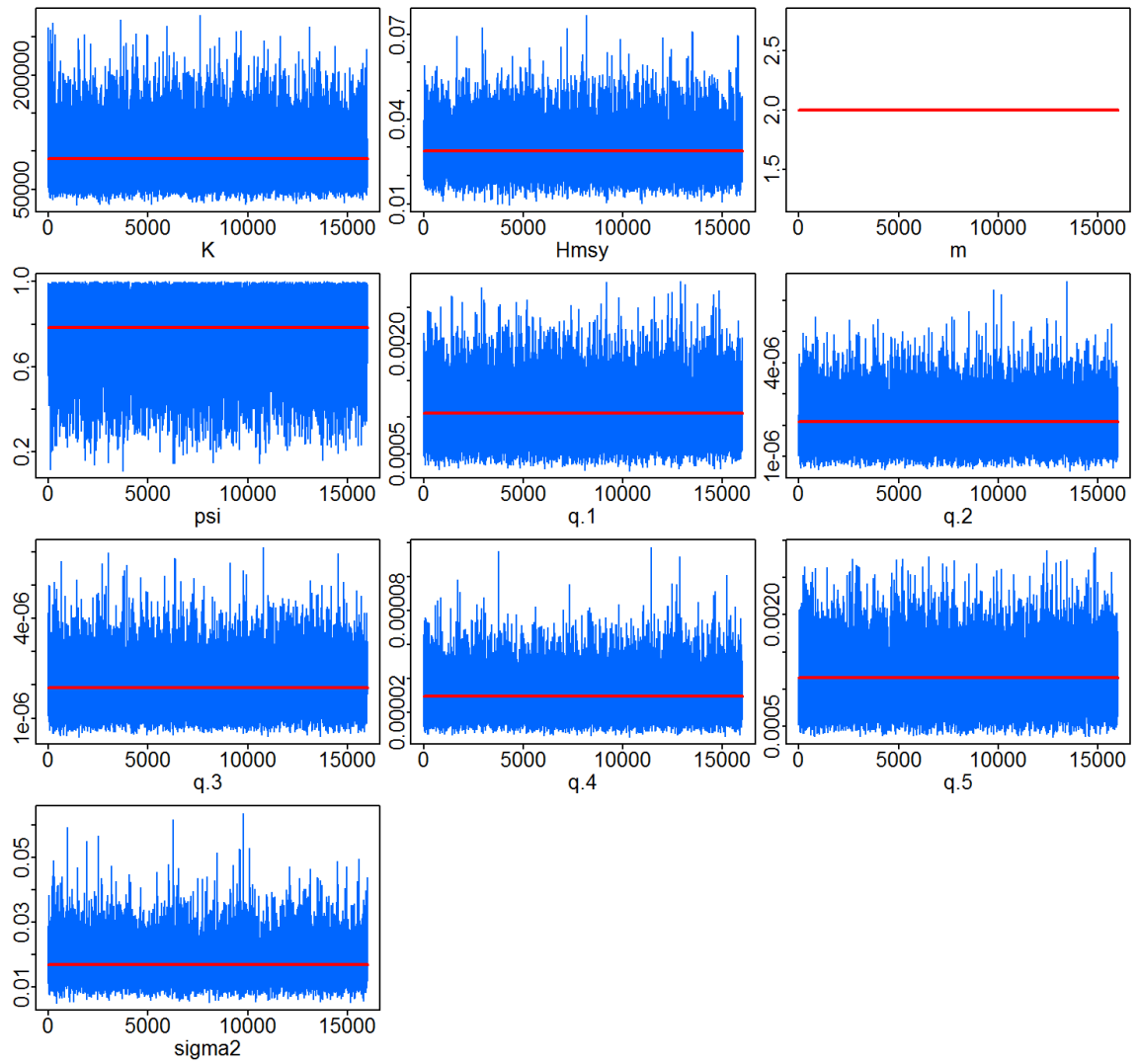
Figure A2. Trace plots for the main model parameter drawn from MCMC samples in the base-case scenario for South Atlantic shortfin mako shark stock assessment.